C20

ATP sensitivity of ATP-sensitive potassium channels in permeabilised β-cells

A. Tarasov, C. Girard and F.M. Ashcroft

Physiology, University of Oxford, Oxford, UK

ATP-sensitive potassium (K_{ATP}) channel closure in response to glucose metabolism links changes in blood glucose concentration to insulin secretion from pancreatic β-cells. K_{ATP} channels are inhibited by ATP (which binds to the Kir6.2 subunit) and activated by Mg-nucleotides such as MgADP and MgATP which interact with the SUR1 subunit. In excised membrane patches, the channel is half-maximally blocked (IC_{50}) by 10-30μM ATP and fully blocked by 1 mM ATP. However, channel activity is observed in on-cell patches on β-cells when $[ATP]_i$ is predicted to be 1-5 mM. This suggests the apparent ATP sensitivity in the excised patch differs from that in intact β-cells, due to loss of cytoskeletal elements or cytosolic modulators such as MgADP or PIP_2, which enhance K_{ATP} channel activity and decrease its ATP sensitivity. To address this issue, we established an open-cell-attached patch-clamp configuration (open-cell) that enables K_{ATP} channel ATP sensitivity to be measured in cell-attached patches on permeabilized cells.

B-cells were isolated from pancreata of humanely killed NMRI mice and cultured for 1-3 days. Single-channel currents were recorded at -60 mV using the open-cell configuration. Cells were permeabilized with 5 μg/ml *S. aureus* α-toxin or 20-30 HU/ml streptolysin O (SLO). The pipette solution contained (mM): 140 KCl, 10 HEPES (pH 7.2 with KOH), 1.1 $MgCl_2$, 2.6 $CaCl_2$. The bath solution contained (mM): 30 KCl, 110 K-aspartate, 0.084 $CaCl_2$, 2 $MgSO_4$, 10 HEPES (pH 7.2 with KOH), 0.5 EGTA and various [ATP]. The Mg^{2+}-free bath solution contained (mM): 30 KCl, 110 K-aspartate, 2.6 $CaCl_2$, 10 HEPES (pH 7.2 with KOH), 0.5 EGTA, 5 EDTA. Data are given as mean±SEM; n is the number of patches.

The ATP sensitivity of the K_{ATP} channel in the open-cell configuration was markedly lower than in the excised patch. The IC_{50} was 101±28 μM (n=6) in open-cell vs 23±2 μM (n=5) in excised patch ($p<0.05$), when permeabilized using α-toxin (cut-off <3 kDa). There was no difference in the open-cell ATP sensitivty when SLO (cut-off 150 kDa) was used for permeabilization (IC_{50} = 109±38 μM (n=7)), suggesting that it is not due to readily diffusible agents of low molecular weight. However, the difference in ATP-sensitivity was abolished in Mg^{2+}-free solution (IC_{50} = 14±4 μM (n=6) in open-cell and 10±1 μM (n=5) in excised patch) or when the poorly hydrolysable ATP analogue, ATPγS, was used (IC_{50} = 7±1 μM (n=6) in open-cell, 5±1 μM (n=5) in excised patch). These data suggest a Mg^{2+}-dependent process underlies the reduction in apparent ATP sensitivity seen in open-cell patches. Possible mechanisms include Mg-nucleotide activation via SUR1, and ATP-dependent generation of PIP_3/PIP_2. A contribution of the latter is suggested, as LY294002 (100μM), which blocks PIP_2 synthesis, reduced the ATP sensitivity in both open-cell and excised patch (IC_{50} = 21±3 μM (n=8) in open-cell, 9±1 μM (n=5) in excised patch).

Where applicable, the experiments described here conform with Physiological Society ethical requirements.

C21

The extent of ATP-sensitive potassium channel block by MgATP correlates with the clinical phenotype caused by gain-of-function KCNJ11 mutations

P. Proks[1], C. Girard[1], A. Gloyn[2], A. Hattersley[2] and F. Ashcroft[1]

[1]University Laboratory of Physiology, University of Oxford, Oxford, UK and [2]Institute of Biomedical and Clinical Science, Peninsula Medical School, Exeter, UK

ATP-sensitive K^+ (K_{ATP}) channels control electrical signalling in diverse cell types by coupling metabolism to transmembrane K^+ fluxes. They comprise pore-forming Kir6.2 and regulatory sulphonylurea receptor (SUR) subunits. Metabolic regulation is mediated by changes in intracellular adenine nucleotides: ATP binding to Kir6.2 inhibits, and interaction of MgATP with SUR, increases, channel activity.

In pancreatic β-cells, K_{ATP} channels mediate glucose-stimulated insulin secretion. Heterozygous (*het*) mutations in Kir6.2 (*KCNJ11*) cause permanent neonatal diabetes alone (PNDM; R201H/C) or in association with developmental delay, muscle weakness, and epilepsy (DEND syndrome; Q52R, V59G, I296L). Functional analysis in the absence of Mg^{2+}, to isolate the effects of ATP on Kir6.2, showed both types of mutation reduce channel inhibition by ATP (Gloyn *et al.*, 2004; Proks *et al.*, 2004). However, in cells, K_{ATP} channel activity is governed by the balance between ATP inhibition via Kir6.2 and Mg-nucleotide stimulation mediated by SUR. We therefore studied the MgATP sensitivity of Kir6.2 mutant channels.

K_{ATP} currents were recorded from *Xenopus laevis* oocytes coinjected with wild-type (*wt*) or mutant Kir6.2 and SUR1 mRNAs. To simulate the *het* state, we used a 1:1 mixture of *wt* and mutant Kir6.2 mRNAs. Macroscopic (or single-channel) currents were recorded by patch-clamping inside-out patches. The pipette solution contained (mM): 140 KCl, 1.2 $MgCl_2$, 2.6 $CaCl_2$, 10 HEPES (pH 7.4). The Mg free internal (bath) solution contained (mM): 107 KCl, 1 K_2SO_4, 10 EGTA, 10 HEPES (pH 7.2). The Mg-containing internal solution consisted of Mg-free solution without K_2SO_4 plus 2mM $MgCl_2$ and MgATP (instead of ATP).

Mg^{2+} caused a small increase (1.9±0.4-fold; n=6) in the IC_{50} (13±1 μM) for ATP inhibition of *wt* channels. In contrast, the IC_{50} for homozygous R201C and R201H mutant channels was dramatically increased: IC_{50} = 2.4±0.2 mM (n=5) and 2.0±0.2 mM (n=6) (23.5±2.9-fold and 6.7±0.8-fold increase) respectively. Mg^{2+} dramatically altered the shape of the dose-response curve of homozygous Q52R, V59G and I296L mutant channels, resulting in a substantial fraction (35-87%) of unblocked current at high MgATP. The fraction of unblocked current in 3 mM MgATP for *het* channels was correlated with disease severity, with V59G(40%)>I296L(32%)>Q52R(27%)>R201C(15%)>R201H(8%). This supports the idea that neonatal diabetes results from an increased K_{ATP} current in β-cells, which reduces electrical activity and insulin secretion. Larger increases in K_{ATP}

current may be required to influence electrical activity in other cell types and cause the neorological symptoms associated with DEND syndrome.

Gloyn AL *et al* (2004). *New Eng J Med* **350**, 1838-1849

Proks P *et al* (2004) *Proc Natl Acad Sci USA* **101**, 17539-17544

Where applicable, the experiments described here conform with Physiological Society ethical requirements.

C22

The N-terminus of RCK1 domain controls Ca^{2+} sensitivity of BK_{Ca} channel gating

J. Cui, G. Krishnamoorthy, J. Shi and D. Sept

Biomedical Engineering, Washington University, St. Louis, MO, USA

Voltage- and Ca^{2+}-activated large conductance K^+ (BK_{Ca}) channels are involved in regulating smooth muscle and neuronal activities. Similar to an archeon Ca^{2+}-activated the K^+ channel, MthK, each of four α subunits of BK_{Ca} may contain two cytosolic RCK domains (RCK1 and RCK2) that form a gating ring. The mechanism of Ca^{2+}-dependent activation of BK_{Ca} may resemble that of MthK, derived from its crystal structure, such that Ca^{2+} binding causes channel opening by pulling between the gating ring and the activation gate in S6 (Jiang et al. 2002). Here we show that the BK_{Ca} homologues mSlo1 and dSlo have different Ca^{2+} sensitivities during activation ($\Delta\Delta G_{Ca}$ in response to $[Ca^{2+}]$ increase from 5.7 to 89 μM for mSlo1: -9.04±0.17 kCal/mol, n=6; for dSlo: -20.04±1.3 kCal/mol, n=4). By comparing structure and function between these two homologues using patch clamp techniques, mutagenesis (Shi & Cui, 2001) and protein dynamic simulations (Sept et al. 2003) we have identified a region in the N-terminus of RCK1 that is responsible for their differences in Ca^{2+} sensitivity (ratio of $\Delta\Delta G_{Ca}$ of a chimeric channel with dSlo background and mSlo1 RCK1 N-terminus vs. mSlo1 is 0.99±0.03, n=5). We found that the two channels may not differ in metal binding sites. Instead, structural differences in the N-terminus of RCK1 cause activation energy to change depending on Ca^{2+} occupancy and activation state. When Ca^{2+} binding sites are empty, this structural domain in dSlo stabilizes the closed conformation more than in mSlo1. On the other hand, when Ca^{2+} binding sites are saturated both channels activate with similar activation energy. Recently, Niu et al. (2004) demonstrated that the gating ring and its linker to S6 behave like a passive spring in the process of BK_{Ca} activation. Our results suggest that the N-terminus of RCK1 acts as the spring component and modulates channel activation. Functional differences between mSlo1 and dSlo may be due to different spring properties of this structure.

Jiang et al. (2002). Nature 417, 515-522.

Shi & Cui (2001). J Gen Physiol 118, 589-605.

Sept et al. (2003). Protein Sci 12, 2257-2261.

Niu et al. (2004). Neuron 42, 745-756.

Where applicable, the experiments described here conform with Physiological Society ethical requirements.

C23

Kir6.2 mutations causing neonatal diabetes provide new insights into Kir6.2-SUR1 interactions

P. Tammaro[1], C. Girard[1], J. Molnes[2], P. Njølstad[3] and F. Ashcroft[1]

[1]University Laboratory of Physiology, University of Oxford, Oxford, UK, [2]Department of Clinical Medicine, University of Bergen, Bergen, Norway and [3]Department of Pediatrics, Haukeland University Hospital, Bergen, Norway

ATP-sensitive K^+ (K_{ATP}) channels, comprised of pore-forming Kir6.2 and regulatory SUR subunits, play a crucial role in regulating insulin secretion from pancreatic β-cells by coupling glucose metabolism to insulin exocytosis. Each Kir subunit is associated with a regulatory sulphonylurea receptor (SUR) subunit, the SUR1 isoform being found in β-cells (Aguilar-Bryan *et al.* 1995). Metabolic regulation of K_{ATP} channel activity is mediated by changes in the intracellular concentrations of adenine nucleotides. Binding of ATP to Kir6.2 inhibits, whereas interaction of MgATP with SUR1 activates, K_{ATP} channels. We tested the functional effects of two Kir6.2 heterozygous (*het*) mutations (Y330C, F333I) that cause permanent neonatal diabetes mellitus (PNDM) (Sagen *et al.* 2004; Vaxillaire *et al.* 2004), by heterologous expression in *Xenopus* oocytes. In a homology model of Kir6.2 (Antcliff *et al.* 2005), both residues lie close to the outer mouth of the ATP-binding site, suggesting that they may impair the channel ATP sensitivity.

K_{ATP} currents were recorded from *Xenopus Laevis* oocytes 1-3 days after injection with wild-type (*wt*) or mutant Kir6.2 and SUR1 mRNA. To simulate the *het* state a 1:1 mixture of *wt* and mutant Kir6.2 mRNA was used. Macroscopic or single channel currents were recorded from inside-out patches with the patch-clamp technique. The pipette solution contained (mM): 140 KCl, 1.2 $MgCl_2$, 2.6 $CaCl_2$, 10 HEPES (pH 7.4) plus various ATP concentrations. The Mg-free internal (bath) solution contained (mM): 107 KCl, 1 K_2SO_4, 10 EGTA, 10 HEPES (pH 7.2). The Mg-containing internal solution consisted of Mg-free solution plus 2 mM $MgCl_2$ and MgATP (instead of ATP).

Both mutations reduced ATP inhibition in the absence of Mg^{2+}: the IC_{50} was 10.6±1.8 (n=10) μM for *wt*, compared to 22.8±4.6 (n=5) μM and 19.7±2.0 (n=6) μM for *het*F333I and *het*Y330C channels, respectively. This effect was greater in the presence of 2 mM Mg^{2+}: IC_{50} were 16.7±2.6 (n=6) μM, 39.0±4.0 (n=6) μM and 116±19 (n=6) μM for *wt*, *het*F333I and *het*Y330C channels, respectively. Single channel studies indicated the Y330C mutation reduced ATP inhibition both by impairing ATP binding and indirectly, by stabilizing the intrinsic open state of the channel. In contrast, F333I channels had *wt* kinetics. The stimulatory effect of MgATP (mediated via SUR1) was greatly enhanced by the F333I mutation, an effect that was abolished by SUR1 mutations which prevent MgATP binding/hydrolysis. For both mutations, K_{ATP} currents in 1-3 mM MgATP were increased. In β-cells, this would decrease electrical activity and insulin secretion, thereby producing neonatal diabetes. These data also demonstrate that region of Kir6.2 in which Y330 and F333I reside influences ATP binding and the mechanism(s) by which SUR1 influences intrinsic gating and MgADP activation.

Aguilar-Bryan L *et al.* (1995). *Science* **268**, 423-426.

Antcliff JF *et al.* (2005) *EMBO J* **24**,229-239.

Sagen JV *et al.* (2004) *Diabetes* **53**, 2713-2718.

Vaxillaire M *et al.* (2004). *Diabetes* **53**, 2719-22.

Where applicable, the experiments described here conform with Physiological Society ethical requirements.

C24

Calcineurin Aα regulates Kir6.1/SUR2B in HEK293 cells through an interaction with protein kinase A

N.N. Orie[1], B.A. Perrino[2], A. Tinker[1] and L.H. Clapp[1]

[1]Department of Medicine, UCL, London, UK and [2]Department of Physiology and Cell Biology, University of Nevada School of Medicine, Reno, NV, USA

ATP-sensitive potassium (K_{ATP}) channels are widely distributed in the body and are activated according to the metabolic state of tissues. An important determinant of the activation state of these channels is the degree of phosphorylation. In smooth muscle, K_{ATP} channels are activated when phosphorylated by protein kinase A (PKA) and deactivated when these residues are dephosphorylated by unknown phosphatases (Clapp et al., 1998). Recently we showed that calcineurin, a calcium-dependent phosphatase which is also known to be functionally coupled to the RII subunit of PKA (Santana et al., 2002), plays a role in the regulation of vascular K_{ATP} channel function (Wilson et al., 2000). We therefore investigated calcineurin regulation of the putative smooth muscle clone, Kir6.1/SUR2B and whether PKA was involved in this channel regulation.

Whole cell currents were recorded in a symmetrical potassium (140 mM) gradient in HEK293 cells stably expressing Kir6.1/SUR2B. The magnitude of currents generated through the K_{ATP} channel was assessed by their sensitivity to 10 μM glibenclamide. Cells were dialysed with solution containing different free calcium concentrations (0, 18 and 36 nM). Currents were recorded following 10-15 minutes dialysis in the absence or presence of constitutively active calcineurin Aa (CnAα, 100 nM) or β (CnAβ,100 nM), or calcineurin inhibitors, cyclosporin A (CsA, 10 μM) and calcineurin auto-inhibitory peptide (CAP, 100 μM). Modulation via PKA was investigated using the inhibitors, N-[2-(p-Bromocinnamylamino)ethyl]-5-isoquinolinesulfonamide 2HCl (H-89, 10 μM) and Rp-2'-O-Monobutyryl-cAMPS (Rp-cAMPS, 100 μM).

The magnitude of glibenclamide-sensitive current (I_{glib}) recorded in Kir6.1/SUR2B cells decreased with increase in the intracellular free calcium concentration; I_{glib} recorded at -80 mV in 0 nM free Ca^{2+} was 93.9 ± 14.6 pA/pF (n=20), in 18 nM free Ca^{2+} was 61.3± 8.4 pA/pF (n=43) and at 36 nM free Ca^{2+} was 26.2± 9.5 pA/pF (n=11) confirming a role for calcium in the channel regulation. The constitutively active CnAα but not CnAβ significantly ($P<0.05$, n=6, t-test) attenuated I_{glib} in the absence of intracellular Ca^{2+}. In addition, CAP increased I_{glib} by 2 fold ($P<0.01$, n=8, t-test) compared with control cells (n=43). Maximum activation of the channels occurred 10-15 min following dialysis of CAP. On the other hand, the PKA inhibitors H-89 (n=8) and Rp-cAMPS (n=5) significantly ($P<0.05$, t-test) decreased I_{glib} in Kir6.1/SUR2B and abolished the increase in current observed with CAP. In summary, our results suggest that CNAα but not CNAβ regulates Kir6.1/SUR2B and that this is achieved by opposing PKA-dependent activation of the channel.

Clapp LH *et al* (1998). *Curr Opin Nephro Hepertens* 7, 91-98.

Santana LF *et al* (2002) *J Physiol* 544, 57-69.

Wilson AJ *et al* (2000) *Circ Res* 87, 1019-1025.

Funded by the Medical Research Council, UK

Where applicable, the experiments described here conform with Physiological Society ethical requirements.

C89

In vitro assay for identifying modulators of Kv channel α-β subunit interactions

S. Stafford[2], R. Ginham[2], A.R. Davies[2], G. Lawton[1], P.R. Boden[1] and R.Z. Kozlowski[2]

[1]*Lectus Therapeutics Limited, PO Box 2299, Bristol, BS99 5YG, UK and* [2]*Department of Pharmacology, School of Medical Sciences, University of Bristol, Bristol, BS8 1TD, UK*

Shaker-type voltage-gated K^+ (Kv1.x) channels are composed of a tetramer of pore-forming α subunits which can associate with regulatory proteins such as the Kvβ subunits to form an α4β4 complex. Cytosolic Kvβ subunits, which interact with Kvα subunits through binding to the T1 domain, have been demonstrated to modify the kinetics of Kv channels. Thus understanding Kvα-β interactions, may offer a novel mechanism to exploit the function of Kv channels for therapeutic benefit. The aim of this study was to develop a robust and sensitive assay to determine the nature of the interaction between rKvα1.1 T1 domains and rKv β1 core proteins to allow subsequent identification of compounds which modulate this interaction. rKvα 1.1 T1 domains and rKv β1 core proteins were expressed in *E. coli* as specific fusion proteins, incorporating biotin carboxyl carrier protein as an affinity tag to the rKv β1 core protein. Purified rKvα 1.1 T1 domains were labelled with Cy3 dye. rKv β1 core proteins were immobilised through biotin-streptavidin interactions in a microwell format, with rKvα 1.1 T1 domains titrated into the microwells to form the basis of a fluorescent-readout protein-protein interaction assay.

In order to optimise the assay, binding kinetics of the interaction between rKvα 1.1 T1 domains and rKv β1 core proteins were defined (analyses derived from Davies *et al.* 1999), see Table 1.

The characterisation of rKvα 1.1 T1 domain - rKv β1 core protein interactions enabled construction of a cell-free displacement assay based in a microplate format. Assay parameters were defined following optimisation of the assay for a 96 well plate format. Throughput in this semi-automated process is 200 compounds per day with assay plate coefficient of variation less than 10% (n > 20).

A compound series was identified that modulated the interaction between rKv α 1.1 T1 domains and rKv β1 core proteins (see Table 2 for the compound series).

In summary, determination of the binding kinetics of the interaction between rKv α1.1 T1 domains and rKv β1 core proteins allowed the construction of a robust, fully scaleable assay that was used to identify compounds that modulate this interaction. Compounds identified within this assay may serve to modulate Kv channel kinetics through a novel mode of action.

K_d (nM)	K_{obs} (min_{-1})	$t_{1/2}$ (min)
105 ± 10	0.026	13.1

Table 1. Binding parameters for interactions between of rKv1.1 T1 domain with rKv β1 core protein (n = 3).

Compound name	IC_{50} (μM)
Calix[4]arene	No inhibition
4-Sulfonic calix[4]arene	36.2 ± 3.5
Calix[6]arene	No inhibition
4-Sulfonic calix[6]arene	3.4 ± 0.7
Calix[8]arene	No inhibition
4-Sulfonic calix[8]arene	4.4 ± 0.5

Table 2. Compound series demonstrated to modulate the interaction of the rKv α/β subunits in the microplate assay format.

Davies ARL, Hardick DJ, Blagbrough IS, Potter BV, Wolstenholme AJ & Wonnacott S (1999). Neuropharmacology 38, 679-690.

Where applicable, the experiments described here conform with Physiological Society ethical requirements.

C90

Crucial role of beta subunits for expression and G protein modulation of N-type calcium channels revealed by mutational analysis of the I-II loop of $Ca_V2.2$

J. Leroy, M. Richards, A.J. Butcher, M. Nieto-Rostro, W.S. Pratt, T. Davies and A.C. Dolphin

Pharmacology, University College London, London, UK

High-voltage activated (HVA) calcium channels are heteromultimers composed of a main pore-forming $Ca_V\alpha1$ subunit associated with auxiliary subunits β and α2δ. The β subunits modulate biophysical properties of the channels and promote the voltage-dependence of modulation of N-type calcium channels by G proteins (Meir et al. 2000). They bind to an interaction site of 18 amino-acids (QQxExxLxGYxxWIxxxE), the alpha-interaction domain (AID), conserved in the I-II loop of the $Ca_V\alpha1$ subunit of all HVA calcium channels. By mutating W391 to A in the AID of $Ca_V2.2$, Biacore experiments confirmed that this amino-acid is essential for β1b subunit binding (Fig. 1), for plasma membrane expression and for modulation of the biophysical properties of $Ca_V2.2$ channels.

Whereas robust currents with 10 mM barium as charge carrier were recorded using the patch-clamp technique on tsA-201 cells co-expressing $Ca_V2.2$ with β1b (−219.5±41 pA/pF at +20 mV ; mean±S.E.M., n=12), co-transfection of $Ca_V2.2$(W391A) with β1b induced small currents (−31.7±7.4 pA/pF at +20 mV ; n=11; $p<0.01$ using an unpaired Student's t test). Moreover, without,β $Ca_V2.2$ produced small but recordable currents (−8.2±1.1 pA/pF at +20 mV ; n=13; $p<0.01$) while no currents were recorded when Ca2.2(W391A) was expressed alone (n=21), suggesting that some endogenous β may be present in tsA-201 cells and trafficking wild type $Ca_V2.2$. We then studied the G protein modulation of these channels by co-expressing a dopamine D2 receptor and activating it with the D2 receptor agonist quinpirole (100 nM). For the wild-type channel, quinpirole induced an inhibition of 53.5±3.8% (n=12; $p<0.01$) of the currents, a +7 mV shift of activation and prepulse potentiation was observed. The $Ca_V2.2$(W391A) mutant was still inhibited (46.4±8% n=11; $p<0.01$) by quinpirole and a positive shift of +6.5 mV for its activation still occurred but no prepulse potentiation was observed for this mutant. In contrast, only the expression of the channel at the plasma membrane was affected when $Ca_V\beta2a$ was co-expressed with this mutant channel, while all the biophysical

properties of the expressed $Ca_V2.2$W391A channels were still normally modulated by the palmitoylated $Ca_V\beta2a$ including the voltage-dependence of G-protein modulation, suggesting another level of modulation by this subunit. These results confirm that the W391 is crucial for β subunit binding to the I-II linker of $Ca_V2.2$, and show that no $Ca_V2.2$ is functional at the plasma membrane in the complete absence of interaction with a β subunit. The results also provide evidence for the role of β subunits in the voltage-dependence of modulation of N-type calcium channels by G protein-coupled receptors.

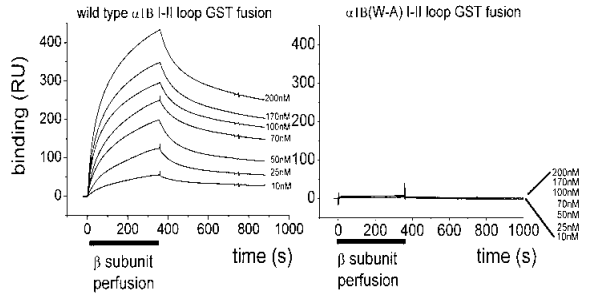

Figure 1: Examples of Biacore 2000 sensorgrams for comparison of purified beta1b binding to a GST- CaV2.2 I-II loop (A) GST- CaV2.2 (W391A) I-II loop (B).

Meir et al. (2000). Biophys J 79, 731-746.

Supported by the Wellcome Trust.

Where applicable, the experiments described here conform with Physiological Society ethical requirements.

C91

Regulation of neuronal voltage-gated sodium and potassium channels by the ubiquitin ligase Nedd4/4-2

J. Ekberg[1], P. Poronnik[1], S. Kumar[2] and D.J. Adams[1]

[1]School of Biomedical Sciences, University of Queensland, Brisbane, QLD, Australia and [2]Hanson Institute, Adelaide, SA, Australia

Nedd4 and Nedd4-2 are ubiquitin-protein ligases that can regulate cell surface levels of membrane proteins by binding C-terminal PY motifs leading to ubiquitination, internalization and lysosomal/proteosomal degradation of the target proteins. Since Nedd4/4-2 are expressed at high levels in neurons, ion channels involved in neuronal excitability are potential targets for this regulation. We examined the regulation of cloned voltage-dependent Na^+ and K^+ channels expressed in *Xenopus* oocytes by Nedd4/4-2. An ovarian lobe was removed from *X. laevis* frogs under anaesthesia. 2-3 days after cRNA injection of defolliculated oocytes, depolarization-activated membrane currents were recorded using the two-electrode voltage clamp technique.

Six of the nine mammalian voltage-gated Na^+ channels (VGSCs) share the PY-motif PPXY. We have recently shown, using *in vitro* ubiquitination and Far Western techniques, that Nedd4/4-2 can bind to and ubiquitinate the neuronal VGSCs $Na_v1.2$, $Na_v1.7$ and $Na_v1.8$. In addition, co-expression experiments in *X. laevis* oocytes demonstrated that both Nedd4 and Nedd4-2 interact with $Na_v1.2$ and $Na_v1.7$, while only Nedd4-2 acts on $Na_v1.8$ (Fotia *et al.* 2004). The co-expression study has now been extended to include $Na_v1.3$, which was found to be down-regulated by both Nedd4 and Nedd4-2 to 31 ± 4 % (n = 23, $P < 0.001$) and 11 ± 2% (n = 24, $P < 0.0001$) of control, respectively.

The muscarine-sensitive K^+ current (M-current), mediated by a heteromeric channel consisting of KCNQ2 and KCNQ3 subunits, plays a key role in regulating neuronal excitability by stabilizing the membrane potential (Peters *et al.* 2005). The intracellular C-terminal tail of KCNQ3 contains the motif PPXPPY, similar to the PY motif in ClC-5 which is regulated by Nedd4-2 (Hryciw *et al.* 2004). KCNQ2/3 was co-expressed with Nedd4-2 in *X. laevis* oocytes, resulting in a pronounced reduction in the K^+ current amplitude (60 ± 5% of control, n = 42; $P < 0.001$), whereas a ligase deficient Nedd4-2 mutant had no effect. When KCNQ2 was expressed alone, Nedd4-2 did not affect K^+ current amplitude, suggesting that the current through KCNQ2/3 can be regulated by Nedd4-2 limiting the availability of the KCNQ3 subunit to the complex.

Fotia AB *et al.* (2004). *J Biol Chem* **279**, 28930-28935.

Peters HC *et al.* (2005). *Nature Neurosci* **8**, 51-60.

Hryciw DH *et al.* (2004). *J Biol Chem* **279**, 54996-5007.

Where applicable, the experiments described here conform with Physiological Society ethical requirements.

C92

Derivatives of pentapeptide QYNAD are processed in cerebrospinal fluid

A. Gontsarova[1], E. Kaufman[3], A. Dressel[2], H. Tumani[4], C. Kunert-Keil[1] and H. Brinkmeier[1]

[1]Institute of Pathophysiology, University of Greifswald, Greifswald, Germany, [2]Department of Neurology, University of Greifswald, Greifswald, Germany, [3]Department of Applied Physiology, University of Ulm, Ulm, Germany and [4]Department of Neurology, University of Ulm, Ulm, Germany

The pentapeptide with the sequence Gln-Tyr-Asn-Ala-Asp (QYNAD) was isolated from cerebrospinal fluid (CSF) of patients with inflammatory demyelinating neurological diseases. QYNAD was shown to inhibit Na^+ currents by shifting the steady-state inactivation curve to more negative potentials. However, this finding was not consistently reproducible in other laboratories. This led to the following hypotheses. First, the efficacy of QYNAD could depend on certain conditions of peptide synthesis or on the presence of still unknown cofactors in CSF. Second, QYNAD could be one factor among a group of related peptides that are targets of enzymatic degradation and modification. The possible influence of cofactors and by-products on the biological activity of QYNAD was studied by whole-cell recordings on HEK 293 cells functionally expressing rat Nav1.2 channels. Further, the possible loss of an additional amino acid that may have occurred during storage of CSF or peptide isolation was investigated. Using highly purified peptides, we did not observe significant effects of QYNAD (100 μM) on Na^+ currents. Permutated peptides (YNQDA), peptides of altered length and charge, tetra- and tripeptides derived from the sequence had no or only slight effects on Na^+ currents. Only peptide mixtures with the sequence XQYNAD (where X is one of 20 L-amino acids) caused a reversible block of rat Nav1.2 channels due to a shift of voltage depend-

ence of activation. We used this peptide mixture, XQYNAD, as a model to study the possible enzymatic degradation of peptides and their modification in CSF. Peptide concentrations were determined by mass spectrometry using an LC/MSD Trap system 1100 Series (Agilent, Germany). Incubation of XQYNAD (100 μM) with 300 μl samples of CSF at 37°C resulted in a release of QYNAD (MW: 609 Da) within several hours and a further conversion to its pyroglutamic acid form (pyQYNAD, MW 592 Da). After 5 h incubation the average QYNAD concentration was 6.6 ± 2.2 μM (n = 27), while the pyQYNAD concentration yielded 5.19 ± 1.86 μM. In the presence of the low MW (< 3 kDa) fraction of CSF neither QYNAD was released nor was the conversion of synthetic QYNAD to pyQYNAD observed. To study the conversion of QYNAD to its pyroglutamic acid derivative more exactly, we incubated QYNAD (10 μM) with CSF samples. Under control conditions 83-90% were converted to pyQYNAD within 5 h. This conversion could be prevented by inhibitors of the enzyme glutaminyl cyclase (EC 2.3.2.59). The addition of benzylimidazole (35.5 or 71 μM) or acetlyhistamine (85.5 or 170 μM) to the samples led to a decrease of pyQYNAD to 38-60% (n = 8) of total detected peptide. We conclude that small peptides underlie dynamic processing in CSF and that these processes are dependent on the high MW fraction of CSF, probably on the activity of an amiopeptidase. The fact QYNAD is converted to its pyroglutamic acid derivative in CSF indicates the presence and activity of glutaminyl cyclase. To clarify the role of QYNAD and related peptides in the pathogenesis of inflammatory demyelinating neurological diseases it will be helpful to study enzymes that degrade and modify peptides in the CSF.

Brinkmeier H, Aulkemeyer P, Wollinsky KH & Rüdel R (2000). Nat Med 6, 808-811.

Cummins TR et al. (2003). Neurology 60, 224-229.

Meuth SG et al. (2003). Eur J Neurosci 18, 2697-2706.

Schilling S et al. (2003). J Biol Chem 278, 49773-49779.

Supported by the European Union.

Where applicable, the experiments described here conform with Physiological Society ethical requirements.

C93

Single channel study of the spasmodic mutation (A52S) in the glycine receptor

A. Plested, P. Groot-Kormelink, L.G. Sivilotti and D. Colquhoun

Pharmacology, UCL, London, UK

In the spinal cord and brainstem, fast inhibitory transmission via glycine receptors controls muscle tone and locomotion. A loss-of-function mutation in the glycine receptor α1 subunit, A52S, gives rise to *spasmodic*, a mouse with a phenotype that resembles human hyperekplexia (startle disease) (1). Synaptic currents are smaller, and decay faster, than normal (2). We expressed rat heteromeric (α1β) receptors with this mutation in human embryonic kidney 293 cells, and recorded single-channel data in the cell-attached configuration (see Fig. 1). The maximum P_{open} for A52S receptors was 97 ± 1% (n = 2-5 patches per point), similar to wild type (3). The EC_{50} for P_{open} was increased by a factor of 5, from 60 μM glycine (3) for wild-type receptors to 326 ± 9 μM (n = 2-5 as before), and the Hill slope was reduced from 3.2 (3) to 1.9 ± 0.1.

Several reaction schemes were fitted to data at three concentrations of glycine (four sets of simultaneous maximum-likelihood fits with HJCFIT (3)). Good fits were obtained using mechanisms in which three glycine molecules could bind to the receptor, and where an extra shut state was included (in addition to the resting and open states) at each level of liganding. Gating efficacy was similar to that of wild-type receptors (the fully-liganded efficacy was about 40 (3)). The apparent strong cooperativity in binding of successive glycine molecules to shut channels in wild type (3) was much less obvious in A52S receptors. Good fits could be obtained with the affinity for all binding reactions fixed at K = 1000 μM. The 'flip' mechanism (3) (see Fig. 1) postulates a physical interpretation of the extra shut states, and a mechanism for the apparent cooperativity. Fits for A52S receptors showed a difference in glycine affinity between the resting and flipped forms of the receptor much smaller than for wild-type receptors ($K_R/K_F \approx 2$ for A52S, compared to 65 for wild type (3)). We conclude that the increase in glycine EC_{50} in the A52S mutation (which is unlikely to be in the binding site) results roughly equally from a decrease in resting affinity, and from the weakening of the conformational change between shut forms of the receptor, so reducing the length of channel activations.

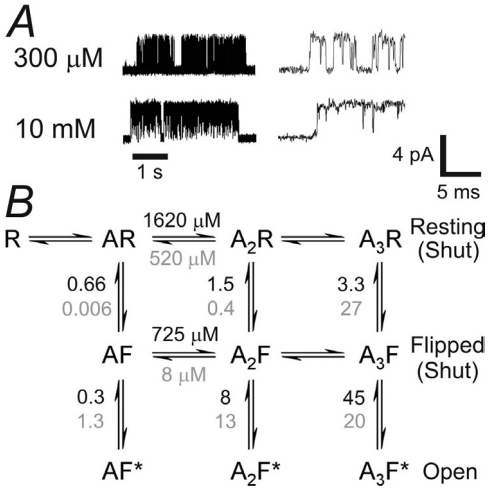

Figure 1. A, typical single A52S glycine receptor activations at 300 μM and 10 mM glycine.

B, the 'flip' model. Equilibrium constants (calculated for the fitted rate constants, vertical ones are the downward rate divided by the upward) are shown for A52S (black) and wild-type (grey). The mutation reduces the affinity of glycine for the flipped state much more than for the resting state, so the increase in glycine affinity after flipping is much smaller.

Ryan et al. (1994). Nature Genetics 7, 131-135.

Callister et al. (1999). Clin Exp Pharm Phys 26, 929-931.

Burzomato et al. (2004). J Neurosci 24, 10924-10940.

Where applicable, the experiments described here conform with Physiological Society ethical requirements.

PC129

Role of monocytic ATP-sensitive potassium channels in the development of stasis-induced blood-borne thrombosis

D. Schmid[2], D.L. Staudacher[1], R. Bueno[1] and P.G. Spieckermann[1]

[1]Center for Physiology and Pathopysiology, Medical University of Vienna, Vienna, Austria and [2]Department of Clinical Pharmacology, Medical University of Vienna, Vienna, Austria

Local hypoxemia occurring in insufficiently flowing blood is an important factor for the development of stasis-induced venous thrombosis, which can potentially cause terminal embolism. The mechanisms by which hypoxemia triggers thrombosis are still incompletely understood. Monocytes are known to adopt procoagulatory properties, upregulation and de-encryption of tissue factor upon activation (Luther et al. 1990; Lawson et al. 1997). Since metabolism sensitive KATP-channels were identified previously on bovine monocytes (Loehrke et al. 1997), the aim of the present study was to investigate the role of KATP-channels on human monocytes for initiating a procoagulatory state under stasis conditions.

Stasis was simulated ex vivo by incubating whole blood of healthy men (n=3) at 37°C in tightly sealed tubes and slight mechanical agitation, while pO2 was deliberately allowed to deplete (pO2 depletion rate: 7% per hour). Tissue Factor Coagulation Time (Santucci et al. 2000) (TiFaCT) in whole blood was measured in quadruples after 2 and 6 h of stasis, in presence of 100 uM KATP-channel blocker glibenclamide or 30 uM KATP-channel opener pinacidil and each of these in presence of 10 ug/ml LPS. TF-expression on CD14- positive monocytes was quantified by flow cytometry (AntiCD142-PE, clone HTF-1, AntiCD14-PerCP, clone mPhiP89).

With increasing time stasis (control) leads to acceleration of TiFaCT (93.43 ± 2.4 and 76.97 ± 1.28 sec after 2 or 6 h, resp.). LPS further stimulated clotting (88.49 ± 3.23 and 64.42 ± 0.66, resp.) In the presence of pinacidil this phenomenon is even further enhanced (83.57 ± 1.92 and 56.3 ± 1.01 sec, resp.). Also pinacidil alone leads to a slightly accelerated clotting (aprox. 10%) after 6 h of stasis compared to control. Glibenclamide inhibits LPS-induced accelerated clotting by 10% after 2h. Glibenclamide alone decelerates clotting by 3% after 6h of stasis.

Flow cytometry shows 1.64 and 2.8% TF positive CD14+ cells after 2 and 8 h of stasis, resp. Pinacidil enhances TF expression in 2.65 and 12.2% of cells, resp. In presence of glibenclamide, 1.55 and 2.3%, resp., of CD14+ cells were TF-positive.

As a preliminary conclusion, KATP-channels seem to be involved in the acceleration of blood clotting under stasis conditions and clearly modulate coagulation in the case of strong concomitant LPS-stimulation. Further studies are necessary to identify molecular identity of the monocytic KATP-channels and to clarify the signalling pathway involved.

Lawson CA et al. (1997). J Clin Invest 99, 1729-1738.

Loehrke B et al. (1997). Pflugers Arch 434, 712-720.

Luther T et al. (1990). Blut 61, 375-378.

Santucci RA et al. (2000). Thromb Haemost 83, 445-454.

Where applicable, the experiments described here conform with Physiological Society ethical requirements.

PC130

ATP-releasing role and spatial distribution of maxi-anion channels in cardiomyocytes

A.K. Dutta[1], R.Z. Sabirov[1], H. Uramoto[1], Y.E. Korchev[2], A. Shevchuk[2] and Y. Okada[1]

[1]Department of Cell Physiology,, National Institute for Physiological Sciences, Okazaki, Aichi, Japan and [2]Division of Medicine, MRC Clinical Sciences Center, Faculty of Medicine,, Imperial College of Science, Technology and Medicine, London, UK

Purinergic signalling plays a crucial role in the physiology of the heart. In the present study, we examined the involvement of maxi-anion channels in ATP release from primary cultures of cardiomyocytes of humanely killed neonatal rats and their distribution pattern on the sarcolemmal surface. Using a luciferin-luciferase assay, it was found that ATP was released to the bulk solution when the cells were subjected to chemical ischaemia, hypoxia or hypotonic stress. The cell surface ATP level of a single cardiomyocyte, measured by a biosensor technique, was found to exceed a micromolar level. Conventional patch-clamp studies showed that all three stimulation induced the activation of single-channel events with a large unitary conductance (390 pS). The pharmacological properties of the swelling-induced ATP release and maxi-anion channel were similar. The channel was selective to anions and showed significant permeability to ATP^{4-} (P_{ATP}/P_{Cl} 0.1) and $MgATP^{2-}$ (P_{ATP}/P_{Cl} 0.16). After taking a 3-D image of the cell by a scanning ion conductance microscopy technique in which a fine-tipped patch pipette was employed as a probe to monitor the cell surface, the same pipette was employed for patching the specified regions on the cells. We found that the density of ATP-conductive maxi-anion channel was higher in the central region of the cell body compared to the cell extensions. These results indicate that maxi-anion channels are distributed on the surface of sarcolemma predominantly near the cell body centre and serve as a pathway for ATP release in hypotonic, hypoxic and ischemic conditions.

Where applicable, the experiments described here conform with Physiological Society ethical requirements.

PC131

The synthesis and sarcolemmal expression of AQP4 water channel protein in isolated skeletal muscle fibres

M. Kaakinen[1], M. Jarvilehto[2] and K. Metsikko[1]

[1]Department of Anatomy and Cell biology, University of Oulu, Oulu, Finland and [2]Department of Biology, University of Oulu, Oulu, Finland

Aquaporins are channel forming proteins, which mediate a rapid transport of water due to the osmotic and hydrostatic pressure gradients. One aquaporin type (AQP4) has also been localized in the skeletal muscle, in which its expression is modulated by changes in muscle use. In this study we examined the sarcolemmal expression pattern and the synthesis of AQP4 in cultivated skeletal muscle fibres.

The muscle fibres were isolated from musculus flexor digitorum brevis (FDB) of humanely killed rats. The isolation was per-

formed by using collagenase treatment. Fibres were cultivated in a CO_2-independent medium (Dulbecco's medium) overnight at 22 ± 1°C with or without Brefeldin-A (5 μg/ml), a drug that prevents transport from the ER to the Golgi elements. The muscle fibres were either immediately fixed with 3% paraformaldehyde or incubated without Brefeldin-A for 2 h at 20°C. The selected temperature prevents transport from the Golgi to plasmalemma (Matlin & Simons, 1983). AQP4 and the Golgi elements were detected immunohistochemically by using AQP4 antibody and an antibody against the endogenous Golgi marker GM-130. Samples were examined using a confocal microscope.

The results revealed that the fraction of FDB fibres harbouring AQP4 varied between 33—47% in different myofibre preparations (n = 4). Moreover, the staining pattern in fibres was not uniform. Typically either one end or both ends of the fibre was stained. Homogenous staining extending throughout the fibre was found only in a fraction of fibres. BFA treatment resulted in a strong staining over z-disks and perinuclear regions extending always from one end of the fibre to the other. This staining pattern corresponds to the exit sites of the myofibre ER (Kaisto & Metsikkö, 2003). The exit site staining was found both in fibres which did not harbour AQP4 at the sarcolemma as well as in fibres in which sarcolemmal expression of AQP4 was present. After the 2 h incubation at 20°C in the absence of BFA, AQP4 was partially colocalized with the GM-130 that exhibited spots around the nuclei and in long rows of spots in the cytosol.

In conclusion, the results revealed that only a fraction of the FDB fibres harboured AQP4 at the sarcolemma and in these fibres the staining pattern was not uniform. This is surprising since FDB consist almost entirely of fast twitch fibre types, in which the expression level of AQP4 should be high. On the other hand, the BFA treatment revealed that in some fibres there exists synthesis of AQP4 despite the fact that the protein is not expressed at the sarcolemma. Moreover, the exit site staining pattern was always uniform throughout the fibre indicating that all the nuclei are equally recruited for the expression of AQP4.

Kaisto T & Metsikkö K (2003). Exp Cell Res 289, 47-57.

Where applicable, the experiments described here conform with Physiological Society ethical requirements.

PC132

Towards the subcellular location of human ClC-6: development of anti-ClC-6 antibody

S. Ignoul[1], F. Jouret[2], O. Devuyst[2] and J. Eggermont[1]

[1]Lab of Physiology, K.U.L, Leuven, Belgium and [2]Lab of Nephrology, U.C.L, Brussels, Belgium

Human ClC-6 is a membrane protein belonging to the ClC chloride channel family which in mammals contains both plasma membrane and intracellular channels. Based on its primary structure ClC-6 is most closely related to ClC-7, a lysosomal chloride channel in mammals. Despite being cloned for nearly a decade, the cellular function(s) and the intracellular distribution of ClC-6 remain largely unknown. The aim of this study is therefore to investigate the expression pattern, the subcellular location and function of the human ClC-6. As a first approach we raised rabbit polyclonal antibodies against a unique region in the COOH-terminus of hClC-6. To test the polyclonal antiserum by Western Blotting, COS-cells were transiently transfected with a hClC-6 expression vector and microsomal membranes were prepared. After SDS-PAGE and Western blotting, immunostaining with the polyclonal antiserum and peroxidase-conjugated secondary antibodies recognised a band of 100 kDa (predicted molecular mass of non-glycosilated hClC-6 is 97 kDa; three independent experiments). Two observations indicate that the immunoreactive band corresponds to hClC-6. First, there was no signal on blots containing microsomes from non-transfected COS-cells. Second, the 100 kDa band was not observed when blots with microsomes of hClC-6 transfected COS-cells were incubated with pre-immune serum and peroxidase-conjugated secondary antibodies. Furthermore, after PNGaseF treatment of microsomes from transfected COS cells we observed a downward shift of the 100 kDa band on Western blot, which indicates that hClC-6 is glycosylated. In a next series of experiments we explored whether affinity-purified anti-hClC-6 antibodies could be used for immunofluorescence with Alexa Fluor dye conjugated secondary antibodies. Immunostaining of COS-cells revealed a fluorescent signal in the perinuclear region of hClC-6 overexpressing COS cells, but no signal in non-transfected wild-type COS cells. In a second series of experiments we have studied the expression pattern of ClC-6 in the mouse kidney by RT-PCR experiments on microdissected fragments of the mouse nephron. This showed a high expression of mClC-6 mRNA in the proximal convoluted part of the proximal tubulus with decreasing levels of expression in the distal parts of the nephron. From these experiments, we conclude that we have generated a polyclonal antibody which recognizes hClC-6 in Western blots and immunofluorescence and that in transiently transfected COS cells hClC-6 occurs as a glycosilated protein that resides in an intracellular, perinuclear compartment.

Where applicable, the experiments described here conform with Physiological Society ethical requirements.

PC133

A difference in H_2O_2 inhibition of the Kir3.1/Kir3.4 and Kir2.1 inward rectifier K^+ channels

S.M. Makary[1], R.N. Leach[2] and M.R. Boyett[1]

[1]Medicine, Manchester University, Manchester, UK and [2]School of Biochemistry and Molecular Biology, University of Leeds, Leeds, UK

Kir3.1/Kir3.4 and Kir2.1 are inward rectifier K^+ channels underlying $I_{K,ACh}$ (ACh-activated K^+ current) and $I_{K,1}$ (background K^+ current) in the heart. Reactive oxygen species such as H_2O_2 are implicated in ischemia/reperfusion injury. We have compared the effect of H_2O_2 on Kir3.1/Kir3.4 and Kir2.1 channels expressed in Xenopus oocytes. Currents were recorded using the two-electrode voltage clamp technique during 750 ms voltage clamp pulses from -130 to +60 mV from a holding potential of 0 mV. Perfusion of 3 mM H_2O_2 for 10 min resulted in a substantial inhibition of Kir3.1/Kir3.4 current but not Kir2.1 current (Fig. 1). Kir3.1/Kir3.4 current was inhibited by 92.3±1.2%, but Kir2.1

current was inhibited by 16.3±4% (mean±SEM; n=5; Kir3.1/Kir3.4 vs Kir2.1, P<0.001, t test). Kir3.1/Kir3.4 current showed reversible inhibition. However, Kir2.1 current showed irreversible inhibition. The reversible inhibition of Kir3.1/Kir3.4 by H_2O_2 argues against irreversible oxidation of the Kir3.1/Kir3.4 channel and suggests another possible mechanism of action. The Kir3.1/Kir3.4 channel has been shown to be suppressed by tyrosine phosphorylation (Rogalski et al. 2000) and H_2O_2 activates tyrosine kinases (Yan & Berton, 1996). Endogenous insulin-like growth factor receptor activation with 2 μM insulin (expected to activate tyrosine kinases) and application of 100 μM 4 methoxyphenacyl Br (tyrosine phosphatase inhibitor) inhibited Kir3.1/Kir3.4 current by 45.0±22.1% and 46.9±6.0%, respectively (n=5). Oocytes expressing the Kir3.1/Kir3.4 channel were incubated with 3 mM H_2O_2 and then homogenised and the detergent soluble fraction was taken for immunoprecipitation with anti-Kir3.1 antibodies. Immunoblotting of immunoprecipitates with anti-phosphotyrosine and anti-Kir3.1 antibodies confirmed the presence of tyrosine phosphorylated Kir3.1 subunits. These observations demonstrate that Kir3.1/Kir3.4 and Kir2.1 channels respond differently to H_2O_2. It is possible that Kir3.1/Kir3.4 is regulated by H_2O_2 via tyrosine phosphorylation. However, Kir2.1 is also known to be inhibited by tyrosine phosphorylation (Wischmeyer et al. 1998). Another explanation is that Kir3.1/Kir3.4 is regulated by H_2O_2 via reversible oxidation of reactive cysteine residues (Zeidner et al. 2001).

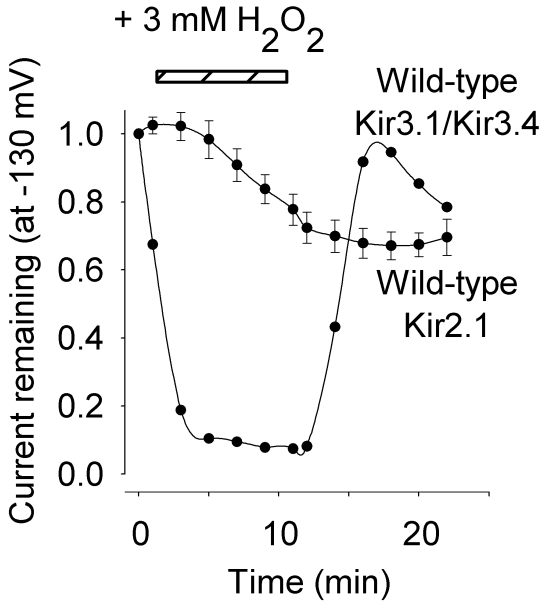

Figure 1. Effect of H_2O_2 on wild-type Kir3.1/Kir3.4 and Kir2.1 channels. Data are means ± S.E.M. (n=5).

Rogalski SL et al. (2000). J Biol Chem 275, 25082-25088.

Wischmeyer E et al. (1998). J Biol Chem 273, 34063-34068.

Yan SR & Berton G (1996). J Biol Chem 271, 23464-23471.

Zeidner G et al. (2001). J Biol Chem 276, 35664-35670.

Where applicable, the experiments described here conform with Physiological Society ethical requirements.

PC134

An integrated look at protein-protein interactions with transient receptor potential channel 4: implications for the control of channel activation

A. Odell, J. Scott and D.F. Van Helden

Biomedical Sciences, University of Newcastle, Callaghan, NSW, Australia

Members of the canonical transient receptor potential (TRPC) family of non-selective cation channels are implicated in the regulation of both store-operated (SOC) and receptor-operated (ROC) Ca^{2+} entry (1). The assembly of TRPC channels into signalling micro-domains is important for the control of channel expression, localization and ultimately activation (2). Disruption of these complexes results in altered Ca^{2+} signalling with potentially deleterious cellular consequences (3). We have investigated the formation of protein complexes with hTRPC4 and their implications for channel function. We demonstrate biochemically, through discontinuous sucrose gradients, that hTRPC4 resides in lipid-raft domains (LRDs) enriched with caveolin-1. 81% of endogenous hTRPC4 in A431 cells (n=6) and 90% of transfected hTRPC4 resides within low-density fractions 3-5 associated with caveolin-1. By comparison, 48% of αII-spectrin (n=11) and approximately 100% of caveolin-1 (n=6) migrate within these fractions. These LRDs are important in the control of channel surface expression, with disruption dramatically increasing the level of hTRPC4 approximately 8-fold (n=5) at the plasma membrane. This internal supply of channels provides a readily releasable pool of hTRPC4 for insertion following stimulation with epidermal growth factor (EGF). We provide evidence that this membrane insertion is accompanied by the dissociation of hTRPC4 from the spectrin cytoskeleton and is driven by the phosphorylation of C-terminal tyrosine residues by Src-family non-receptor tyrosine kinases (STKs). In agreement, the STK members Fyn and Lyn were shown to co-immunoprecipitate with TRPC4 from rat brains of humanely killed rats and COS-7 cells, respectively. The phosphorylation of hTRPC4 also enhanced its association with the scaffolding protein, Na^+/H^+ exchanger regulatory factor, NHERF. We speculate that this association is responsible for the recruitment and stabilisation of hTRPC4 channels at the plasma membrane following EGF application. Furthermore, the phosphorylation of hTRPC4 by STKs is critical for the maintenance of EGF-stimulated Ca^{2+} entry in HEK293 cells stably expressing hTRPC4. The expression of hTRPC4 increased Ca^{2+} influx 2-fold (70.5nM, n=7) when compared to control GFP-expressing cells (35.1nM, n=5) following EGF stimulation. The application of 5μM PP2 prior to EGF stimulation prevented this increase (31.4nM, n=4). Taken together, these data demonstrate the formation of functional hTRPC4 signalling complexes consisting of channels, spectrin, NHERF, and non-receptor tyrosine kinases. These complexes reside in LRDs and are activated by growth factor receptor stimulation to initiate Ca^{2+} influx.

Venkatachalam K, van Rossum DB, Patterson RL, Ma H-T & Gill DL (2002). Nat Cell Biol 4, E263-E272.

Clapham DE, Runnels LR & Strübing C (2001). Nat Rev Neurosci 2, 387-396.

Hong YS et al. (2002). J Biol Chem 277, 33884-33889.

Where applicable, the experiments described here conform with Physiological Society ethical requirements.

PC135

Stimulation of calcium channel function by $\alpha_2\delta$-2 requires its metal ion-dependent adhesion (MIDAS) site

F. Heblich, C. Canti, J. Wratten, I. Foucault, M. Nieto-Rostro, D. Anthony, L. Douglas and A. Dolphin

Pharmacology, University College London, London, UK

In this study we have investigated properties of the membrane-anchored, but predominantly extracellular $\alpha_2\delta$ subunit of voltage-gated Ca^{2+} channels. The $\alpha_2\delta$-1 and $\alpha_2\delta$-2 subunits enhance current amplitude, increase the rate of inactivation and hyperpolarize the steady-state inactivation of high voltage-activated (HVA) currents, although their mechanism of action is not well understood. All $\alpha_2\delta$ subunits contain a Von Willebrand factor-A (VWF) domain within the extracellular α_2 moiety. VWF domains are present in integrins and other proteins, and contain a sequence motif representing a metal ion-dependent adhesion site (MIDAS) which confers divalent metal (usually Mg^{2+})-dependent binding to the ligand.

tsA-201 and NG108-15 cells were transiently transfected using FuGENE. Green fluorescent protein was included to identify transfected cells. Where appropriate, solutions were designed to inhibit unwanted conductances. Data are displayed as % of control, mean ± S.E.M.

We examined the role of the VWF domain in $\alpha_2\delta$-2 and in particular the importance of the MIDAS site in its functional effects. Whole-cell patch-clamp recordings from $Ca_V1.2$ and $Ca_V2.2$ channels, expressed in tsA-201 cells (H_P = -90 mV, 10 mM $BaCl_2$), demonstrate that deletion of the VWF domain and more specifically mutation of the three key amino acids responsible for divalent metal binding in the VWF domain ($\alpha_2\delta$-2 μMIDAS), completely prevented the $\alpha_2\delta$-2 -induced enhancement of these calcium channel currents. For example, peak $Ca_V2.2$ currents expressed with wild type $\alpha_2\delta$-2 were significantly increased to 520 ± 169% of the control in the absence of $\alpha_2\delta$-2 (n = 10) whereas $Ca_V2.2$ currents expressed with $\alpha_2\delta$-2 μMIDAS were unchanged at 111 ± 29% of control (n = 11). Similar results were obtained using Na^+ as charge carrier through $Ca_V2.2$ channels (in the absence of any extracellular divalent cations; $Ca_V2.2$ (n = 25), $\alpha_2\delta$-2 (n = 17), $\alpha_2\delta$-2 μMIDAS (n = 17)). Therefore, any involvement of the MIDAS site binding of Ca^{2+} or Mg^{2+}, in the function of $\alpha_2\delta$-2, in relation to $Ca_V\alpha1$ subunit expression or function, is likely to be during channel assembly or trafficking to the membrane, rather than once the channel has reached the cell surface. Furthermore, although the wild type $\alpha_2\delta$-2 enhanced endogenous HVA calcium currents (n = 13) in differentiated NG108-15 cells ($BaCl_2$ 20 mM, H_P = -40 mV) to 209 ± 39% of control (n = 13), the $\alpha_2\delta$-2 μMIDAS construct had no significant effect, the current being 92 ± 16% of control (n = 12).

Both immunocytochemical and cell surface biotinylation experiments show that these mutations in $\alpha_2\delta$-2 do not prevent their expression at the cell surface. Our future experiments will aim to determine how the mutations in the MIDAS site affect calcium channel function.

This work was supported by the MRC.

Where applicable, the experiments described here conform with Physiological Society ethical requirements.

PC136

An endogenous inhibitor of inward rectifier potassium channels?

A. Collins

Pharmaceutical Sciences, Oregon State University, Corvallis, OR, USA

Reduced activity of inward rectifier potassium channels contributes to an increased risk of arrhythmia in heart failure (Pogwizd et al., 2001). Understanding the regulation of these channels may therefore provide a basis for the development of novel antiarrhythmic agents. Mitochondria are increasingly recognized as a source of important signaling molecules, and we recently reported evidence for an inhibitor of inward rectifier potassium channels that is generated by the action of the mitochondrial uncoupler, carbonyl cyanide p-trifluoromethoxyphenylhydrazone (FCCP) (Collins et al., 2005). To gain further support for the concept of an endogenous inhibitor, we prepared extracts from homogenized *Xenopus* oocytes and tested them for inhibitory activity. Oocytes were homogenized in 4-6.5 ml/g of (mM) 40 KCl, 46 K-gluconate, 5 KF, 0.1 NaVO3, 10 K-pyrophosphate, 1 EGTA, 10 EDTA, 0.1 spermine, 20 HEPES, pH 7.4 with KOH (150 mM final [K+]) (FVPPE) with a Polytron-type or Dounce homogenizer. Homogenates were centrifuged twice at 1000xg, 4 degrees C and the supernatant was retained each time. The supernatant was centrifuged again at 16,000xg, 4 degrees C for 20 minutes, and this supernatant was further centrifuged at 200,000xg, 4 degrees C for 1 hour to pellet the membrane fraction. Alternatively, oocytes were fractionated directly by centrifugation at 16,800xg, 4 degrees C, and the cytoplasmic fraction was diluted into 0.8 ml/g (original oocyte weight) FVPPE. This sample was centrifuged at 200,000xg, 4 degrees C for 1 hour, and the supernatant was further diluted by 8-fold into FVPPE. Complementary RNA for the inward rectifier potassium channel Kir2.2 was transcribed *in vitro* and injected into isolated *Xenopus* oocytes. Two to five days later, inward rectifier currents were recorded in giant membrane patches (Hilgemann, 1995). The pipettes and recording chamber contained FVPPE. Inside-out patches were perfused with FVPPE and with oocyte extracts. Kir2.2 current was inhibited by the 1000xg (3 patches), 16,000xg (4 patches) and 200,000xg (8 patches) supernatants of the Polytron-type or Dounce homogenates, but not by the supernatant from the centrifugation-fractionated oocytes (3 patches). The 200,000xg homogenate supernatant was filtered through Centricon columns with molecular weight cutoffs of 100, 30 and 10kD and the filtrates were tested for their ability to inhibit Kir2.2 current in inside-out patches. All three filtrates inhibited the current. Based on these data, we propose that *Xenopus* oocytes have an endogenous inhibitor of inward rectifier potassium channels that is released from an intracellular compartment by homogenization but not by centrifugation-fractionation, and has a molecular weight of less than 10kD.

Collins A, Wang H & Larson M (2005). Mol Pharmacol Jan 4; [Epub ahead of print].

Hilgemann D (1995). The Giant Membrane Patch. In Single-channel recording, 2nd Edition. Eds. Sakmann, B, Neher, E. pp 307-327.

Pogwizd SM, Schlotthauer K, Li L, Yuan W & Bers DM (2001). Circ Res 88, 1159-67.

American Heart Association

Where applicable, the experiments described here conform with Physiological Society ethical requirements.

PC137

Genistein, but not genistin blocks recombinant $Ca_v3.1$ calcium channel expressed in human embryonic kidney-293 cells

L. Lacinova and M. Kurejova

Institute of Molecular Physiology and Genetics Slovak Academy of Sciences, Bratislava, Slovakia

Conflicting reports on modulation of T-type calcium channels by protein tyrosine kinases (PTKs) have been published. In mouse spermatogenic cells inhibition of PTK by tyrphostin enhanced the current through the T-type calcium channels (Arnoult *et al.* 1997). In contrast, in NG108-15 cells inhibition of PTKs by genistein, lavendustin and herbimycin suppressed current amplitude (Morikawa *et al.* 1998). We have tested the effect of the PTK inhibitor genistein and its inactive analogon genistin on recombinant $Ca_v3.1$ (T-type) calcium channels permanently expressed in human embryonic kidney-293 cells. Calcium currents through the expressed channels were measured in whole cell patch clamp. External solutions contained (mmol/l): 2 $CaCl_2$, 155 NaCl, 5 CsCl, 1 $MgCl_2$ and 10 Hepes; pH 7.4 with NaOH. Internal solution contained (mmol/l): 130 CsCl, 5 $MgCl_2$, 10 TEACl, 5 NaATP and 10 Hepes; pH 7.4 with CsOH. Stock solutions (10 mmol/l) of genistein and genistin were prepared in DMSO. Final concentration of vehicle in experimental solutions was 0.5%. All values are given as mean ± S.E.M. Significance of the difference between two datasets was tested by paired and unpaired Student's t test, as appropriate.

During cell perfusion with internal solution with 0.5% DMSO, run-down of 8.0±3.7% (n=13) calcium current amplitude was observed over the time span of 12-15 min. This minor run-down was not affected by the presence of 0.5% DMSO in external solution. Extracellular application of 50 μM of genistein inhibited current amplitude by 74.8±3.4% (n=11). The effect developed slowly over the time span of 200-220 s and it was only partly reversible. Amplitude inhibition was accompanied by an acceleration of current inactivation from 13.7±1.0 ms to 11.2±0.7 ms (n=6; $p<0.001$) and a deceleration of current activation from 0.96±0.06 ms to 1.45±0.08 ms (n=7; $p<0.001$). Both effects were fully reversible. While the acceleration of inactivation had a similar time course as the amplitude inhibition, deceleration of activation developed more rapidly and saturated after approximately 80 s. During intracellular application of 50 μM of genistein current amplitude was decreased by 10.4±1.1% (n=10). This decrease was not significantly different from run-down observed in cells perfused by vehicle alone. 50 μM of genistin (genistein, 7-*O*-β-D-glucopyranoside) had no significant effect on current amplitude and kinetics whether it was applied extracellularly or intracellularly.

We suggest that genistein inhibits $Ca_v3.1$ channel by a PTK-independent mechanism. This is supported by the evidence that genistein acted from outside the cell and remained ineffective when applied intracellularly. Because of its effects on current kinetics, interaction of the drug with the channel may be more complex than simple occlusion of conductive pore. Ineffectiveness of its analogon genistin could be explained by the different size of this molecule.

Arnoult T C *et al.* (1997). *EMBO J* **16**, 1593-1599.

Morikawa H *et al.* (1998). *Pflugers Arch* **436**, 127-132.

Supported by Volkswagen Stiftung, VEGA 4/4009/24 and APVT-51-013802.

Where applicable, the experiments described here conform with Physiological Society ethical requirements.

PC138

Breast cancer (human): enhancement of invasiveness by epidermal growth factor via voltage-gated Na^+ channel activity *in vitro*

H. Pan and M.B. Djamgoz

Biological Sciences, Imperial College London, London, UK

Previous work showed that voltage-gated Na^+ channels (VGSCs) are expressed in strongly metastatic human breast cancer (mBCa) MDA-MB-231 cells and that their activity potentiates motility, endocytosis and invasion, involved in the metastatic cascade (Fraser et al. 2002, 2005; Roger et al. 2003). In the present study, we have investigated a possible functional relationship between epidermal growth factor (EGF), well known to be associated with mBCa (e.g. Atalay et al. 2003), and VGSC expression.

MDA-MB-231 cells were cultured in serum-free media for 24 h, then seeded into 12 μm-pore transwell plates and treated with EGF (50 or 100 ng/ml) and/or tetrodotoxin (TTX) (0.2 or 10 μM) for 6-8 h. Transverse migration was quatified using tetrazolium MTT assay; lateral motility (over 24 h) was measured by wound-heal assay (Fraser et al. 2005). Each experiment was performed 4-8 times. Data are presented as mean ± S.E.M.; statistical significance was evaluated using Student's t test.

TTX (10 μM) reduced migration by 33 ± 8% ($p<0.05$; n=8); 0.5 μM TTX had no effect, consistent with underlying potentiation by Nav1.5 activity. An inhibitor of EGF receptor tyrosine kinase, AG1478 (10 μM), reduced motility by 13 ± 2% ($p<0.05$; n=4), indicating involvement of endogenous EGF in motility. Exogenous EGF significantly increased migration by 44 ± 4% (50 ng/ml) and 73 ± 7% (100 ng/ml) ($p< 0.05$ for both; n=8). The effect of exogenous EGF was blocked by AG1478 and by co-application with TTX. Thus, EGF (50 ng/ml) + TTX (10 μM) decreased migration by 18 ± 4% ($p< 0.05$ cf. control; $p<0.001$ cf. EGF-treated; $P>0.05$ cf. TTX-treated; n=8).

It is concluded that VGSC activity plays a significant intermediary role in EGF-induced potentiation of metastatic cell behaviour in human BCa in vitro.

Atalay G et al. (2003). Ann Oncol 14, 1346.

Fraser SP et al. (2002). Breast Cancer Res Treat 76, S142.

Fraser SP et al. (2005). Clin Cancer Res (in press).

Roger S et al. (2003). Biochim Biophy Acta 1616, 107-111.

This study was supported by an Amber Fellowship (PCRF) to H.P.

Where applicable, the experiments described here conform with Physiological Society ethical requirements.

PC139

Auto-regulation of voltage-gated sodium channel protein expression in a strongly metastatic human breast cancer cell line: functional consequences

A. Chioni and M.B. Djamgoz

Biological Sciences, Imperial College London, London, UK

Voltage-gated Na+ channel (VGSC), predominantly neonatal Nav1.5 (nNav1.5), activity can potentiate a variety of cellular behaviours involved in the metastatic cascade (Fraser et al.,2005). We have shown previously that the strongly metastatic human breast cancer (BCa) MDA-MB-231 cells express VGSC α-subunit (VGSCα) protein both in plasma membrane (PM) and intracellularly (Chioni and Djamgoz, 2005). In the present study, we determined if VGSC expression involved self-regulation.

Western blots and confocal microscopy identified VGSC α protein and its subcellular location (quantified by confocal densitometry) in MDA-MB-231 cells. A novel polyclonal antibody specific for nNav1.5 was used (Chioni et al, 2005). Proliferation, transwell migration and matrigel invasion were measured as before (Fraser et al.,2005). Cells were treated with TTX (1-10 μ)M in normal medium. Data are presented as mean ± SEM; paired t-test was used in statistical analyses.

Under normal conditions, migrated cells were seen to express noticeably more VGSC protein, compared with non-migrated cells. Treatment with TTX (up to 10 μM) for 48 hours had no effect on total VGSC? protein expression. However, 10 μM TTX decreased nNav1.5 protein in PM by 46 ±3 % ($p<0.01$; n=3 experiments/100 cells). Treatment with TTX (10 μM; 48 h) during assaying decreased invasiveness of MDA-MB-231 cells by 49 ± 10 % (n=9; $p<0.001$). TTX also reduced migration in a dose-dependent way. Thus, 5 μM TTX reduced MDA-MB-231 cell migration by 31 ± 10 % (n= 7; $p<0.05$); 1 μM TTX had no effect (n= 6; $p>0.05$). The effect of pre-treating the cells with TTX (10 μM; 48 h) was studied in migration assays. TTX pre-treatment reduced migration by 55 ± 8 %, compared with non-pre-treated cells (n=6; $p<0.05$). TTX (10 μM) reduced migration of non-pre-treated cells by 42 ± 5 % (n=7; $p<0.001$) but had no effect on the pre-treated cells ($p>0.05$; n=6). TTX had no effect on proliferation of pre-treated or non-pre-treated cells.

These results are consistent with auto-regulation of functional VGSC expression in MDA-MB-231 cells. Thus, blocking VGSC activity with TTX would induce trafficking of nNav1.5 protein from PM into the cell, leading to suppression of metastatic cell behaviour.

Chioni AM & Djamgoz MBA (2005). J Physiol Kings College meeting.

Chioni et al. (2005). Submitted.

Fraser et al. (2005). Submitted.

Fraser SP et al. (2002). Breast Cancer Res Treat. 76 (Suppl 1), S142.

Grimes JA et al. (1995). FEBS lett. 369, 290-294.

A-MC was supported by an Amber Fellowship (PCRF).

Where applicable, the experiments described here conform with Physiological Society ethical requirements.

PC140

Sodium butyrate downregulates calcium-activated potassium channel expression and calcium-activated anion secretion in the Calu-3 human airway epithelial cell line

J. Roy[1], E.M. Denovan-Wright[2], P. Linsdell[1] and E.A. Cowley[1]

[1]Physiology & Biophysics, Dalhousie University, Halifax, NS, Canada and [2]Pharmacology, Dalhousie University, Halifax, NS, Canada

Cystic fibrosis (CF) is a lethal, autosomal recessive disease, caused by mutations in the gene encoding the cystic fibrosis transmembrane conductance regulator (CFTR) Cl^- channel. The most common mutation is ΔF508-CFTR, which is associated with inefficient trafficking of the mutant CFTR protein from the endoplasmic reticulum to the plasma membrane. However, because ΔF508-CFTR retains some functionality as a Cl^- channel, therapeutic efforts have been aimed at increasing the amount of ΔF508-CFTR present in the cell membrane using agents such as sodium butyrate. In this study, we examined the effects of culturing a human airway epithelial cell line, the Calu-3 cell line, in the presence of sodium butyrate (5 mM; between 0 to 96 hours). Calu-3 cells are a model of the submucosal gland serous cell, which normally express a large amount of CFTR, and have been implicated in the pathogenesis of CF pulmonary disease. When grown as monolayers, these cells exhibit basal anion secretion, further stimulated by elevation of intracellular cAMP or Ca^{2+}. We report that, over the time period investigated, butyrate treatment causes a significant decrease in Ca^{2+}-activated Cl^- secretion, measured as the change in transepithelial short circuit current in response to the Ca^{2+} elevating agent thapsigargin (control = 153.8 ± 2.1 μA cm^{-2} (mean ± S.E.M.) (n = 3); 96 h butyrate = 7.9 ± 4.3 μA cm^{-2} (n = 3); $P < 0.0001$, two-tailed t test). Additionally, there is a corresponding loss of response to the secretagogue 1-EBIO, an agent which activates the intermediate conductance, Ca^{2+}-activated basolateral K^+ channel encoded by KCNN4. Initial baseline short circuit current also decreased over the same period of time (from control value of 35.6 ± 3.4 μA cm^{-2} (n =3) to 6.6 ± 0.03 μA cm^{-2} (n = 4) following 96 h butyrate treatment; $P < 0.001$). Quantitative PCR revealed that these losses of response are associated with dramatic decreases in the level of mRNA for both KCNN4 and CFTR. These results suggest that prolonged exposure to sodium butyrate results in a significant down-regulation of KCNN4 and CFTR gene expression, and most importantly, a functional loss of Ca^{2+}-stimulated transepithelial anion secretion. However, since only wild type CFTR was studied, we cannot preclude the possibility that butyrate may have different effects on the expression of ΔF508-CFTR. Furthermore, we suggest that the major component of basal transepithelial anion secretion in unstimulated Calu-3 cells is supported by basal KCNN4 channel activity. Therefore, long term exposure to sodium butyrate may ultimately exacerbate rather than ameliorate the anion secretory deficit seen in CF, especially in tissues that normally exhibit Ca^{2+}-activated anion secretion.

This work was supported by the Nova Scotia Lung Association (to E.A.C.) and the Canadian Cystic Fibrosis Foundation (to P.L.).

Where applicable, the experiments described here conform with Physiological Society ethical requirements.

PC141

Tachykinin receptor-mediated inhibition of $GABA_A$ currents in parvocellular neurones of the rat paraventricular nucleus

M. Womack and R. Barrett-Jolley

Dept. Preclinical Veterinary Sciences, University of Liverpool, Liverpool, UK

The paraventricular nucleus of the hypothalamus (PVN), is central to integration of the cardiovascular response to psychological stress. Furthermore, $GABA_A$ receptor expressing parvocellular PVN neurones are believed to be fundamentally important to this response. Tachykinins are known modulators of $GABA_A$ receptors [3]. During psychological stress brain tachykinin concentrations increase and have been linked to the resulting tachycardia and increase in blood pressure [2]. Tachykinin receptors may, therefore, offer a useful target for future therapeutic intervention in stress-related heart disease. In a previous study, we reported substance P (SP), a member of the tachykinin family, to inhibit the $GABA_A$ receptor currents of spinally projecting parvocellular neurones [1]. All three tachykinin receptor subtypes (NK1, 2 and 3) are sensitive to SP and have previously been identified in the hypothalamus. Each of these receptors is therefore a potential candidate for the inhibition of $GABA_A$ currents by SP. In this study, we sought to identify the tachykinin receptors involved with modulation of $GABA_A$ receptors of anatomically and morphologically identified parvocellular neurones in the rat PVN.

Methods were similar to those described elsewhere [4]; briefly; 14-16 day rats were humanely killed, hypothalami removed to iced artificial cerebrospinal fluid (ACSF) and 250μm sections cut. For whole-cell experiments, neurones were held at -60mV and superfused at 2ml/min with 34-36°C modified ACSF. GABA was applied by pressure ejection. Drugs were added to the superfusing ACSF. Mean data are presented ±S.E.M.

GABA (300μM) evoked whole-cell currents in the range of 0.1-5 nA. These reversed near to ECl and were inhibited by bicuculline (10μM, residual current 13±5%, n=5), confirming these to be $GABA_A$ currents. GABA current amplitudes were decreased to 23±10% (n=5, $p \leq 0.005$, t test) by SP (1μM). Neither NKA4-10 (1μM), NKB (1μM) nor the selective NK3 agonist senktide (1μM) had a significant effect on GABA currents (75.8±6%, n=7; 92±3%, n=4; and 83±11%, n=8, respectively). In the presence of the NK1/2 antagonist spantide (1μM), SP no longer significantly inhibited GABA currents (119±9%, n=3).

In this study, we report the inhibition of GABA currents by SP, but not by the NK3 selective agonists senktide or NKB. These data suggest the involvement of NK1 receptors in the modulation of $GABA_A$ currents by SP.

Barrett-Jolley R. (2003). British Neurosci Abs 17, 33.

Culman J & Unger T (1995). Can J Physiol Pharmacol 73, 885-891.

Yamada K et al. (1996). Kurume Med J 43, 171-175.

Zaki A & Barrett-Jolley R (2002). Br J Pharmacol 137, 87-97.

This work was funded by the BHF, UK.

Where applicable, the experiments described here conform with Physiological Society ethical requirements.

PC142

Contrasting effects of the antipsychotics clozapine and haloperidol on K^+ channels in rat pancreatic beta-cells

L.C. Best[1], A.P. Yates[1] and G.P. Reynolds[2]

[1]Medicine, University of Manchester, Manchester, UK and [2]Mental Health, Queens University Belfast, Belfast, UK

Antipsychotic drugs are known to cause a number of adverse metabolic side effects, including diabetes mellitus. These side effects could be due to impaired islet cell function. We have studied the effects of the atypical antipsychotic clozapine and of the conventional drug haloperidol on electrical and secretory activity in rat pancreatic beta-cells. Islets of Langerhans were isolated from adult Sprague-Dawley rats (killed humanely) by collagenase digestion and dispersed into single cells by brief incubation in a calcium-free medium. Electrical activity and total K^+ conductance were recorded using the perforated patch technique (Best et al. 2004) and single K^+ channel activity in cell-attached patches (Sheader et al. 2001). Insulin release was measured by radioimmunoassay using intact islets (Best et al. 2004).

In the presence of 4 mM glucose, 5 μM clozapine had little or no effect on membrane potential, but hyperpolarised the cell membrane potential in the presence of 16 mM glucose, resulting in a complete inhibition of electrical activity. In contrast, 5 μM haloperidol caused a marked depolarisation of the membrane potential in the presence of low or high concentrations of glucose. In the presence of 10 mM glucose, clozapine increased beta-cell input conductance from 0.59 ± 0.09 to 1.13 ± 0.17 nS (both n=11, $p<0.01$ by paired t test). In contrast, haloperidol reduced input conductance in the absence of glucose from 3.48 ± 0.81 to 1.62 ± 0.20 nS (n=5, $p<0.05$ by paired t test). Cell-attached recordings indicated that these effects were due, at least in part, to changes in K_{ATP} channel activity. Thus, in the presence of 2 mM glucose, channel open probability was increased by clozapine from 0.43 ± 0.06 (n=8) to 0.59 ± 0.06 (n=4, $p<0.01$ by paired t test) and reduced by haloperidol to 0.04 ± 0.04 (n=4, $p<0.001$ by paired t test).

In the presence of 4 mM glucose, neither drug significantly affected insulin release. In the presence of 16 mM glucose, secretion was increased 7.5-fold. Under such conditions, clozapine significantly ($p<0.05$) inhibited insulin release by approximately 40%, whereas haloperidol had no significant effect. We conclude that clozapine and haloperidol exert contrasting actions on electrical activity in rat pancreatic beta-cells as a result of opposing effects on K^+ permeability.

Best L, Yates AP, Decher N, Steinmeyer K & Nilius B (2004). Eur J Pharmacol 489, 13-19.

Sheader EA, Brown PD & Best L (2001). Mol Cell Endocrinol 181, 179-187.

Where applicable, the experiments described here conform with Physiological Society ethical requirements.

PC143

Alternative splicing generates a smaller assortment of $Ca_V2.1$ transcripts in rat cerebellar Purkinje cells than in the cerebellum

M.M. Usowicz, S. Kanumilli, E.W. Tringham, C.E. Payne and K. Venkateswarlu

Pharmacology, University of Bristol, Bristol, UK

The pore-forming $Ca_V2.1$ subunit of P/Q-type Ca channels is encoded by the *Cacna1a* gene. Human, rat and mouse cDNA and genomic analysis have determined that this gene undergoes alternative splicing at multiple loci. However, it is unclear how $Ca_V2.1$ splicing differs between brain regions or cell-types or species. For instance, the P-type Ca channel current described in rat cerebellar Purkinje cells is the prototypical current against which putative P-type currents are compared, and yet the full range of $Ca_V2.1$ splice variants in rat cerebellar Purkinje cells is not known. We used RT-PCR and single-cell RT-multiplex PCR to examine $Ca_V2.1$ alternative splicing in adult rat cerebellum and in single Purkinje neurons. Splice sites in rodent $Ca_V2.1$ genes were identified by aligning rat and mouse $Ca_V2.1$ cDNA sequences. PCR primers were designed to detect the following splicing events: use of different acceptor/donor pairs at the 5′ end of exon (e) 10, inclusion or exclusion (-) of e31a or e43 or e44, coincident exclusion of e33, e36 and e37 (-e33/-e36/-e37) or e43 and e44 (-e43/-e44), mutually-exclusive expression of e37a and e37b, extension or shortening of the 5′ end of e47, and deletion of ~150 nucleotides from e47. RT-PCR was carried out with mRNA extracted from the cerebellar vermis of mature male Wistar rats (6-7 weeks) or on cell contents harvested into a patch-pipette during whole-cell voltage-clamp of Purkinje cells located in a cerebellar slice. Donor rats were humanely killed.

Analysis of PCR products confirmed that the adult rat cerebellum expresses multiple $Ca_V2.1$ transcript variants. However, not all splicing events investigated were detected. These include -e33/-e36/-e37, which occur in a rat pancreatic variant (Ligon et al., 1998) and -e43 or -e43/-e44, which occur in human cerebellar variants (Soong et al. 2002). Furthermore, some cerebellar transcripts are generated by combinations of splicing events not previously described for rat $Ca_V2.1$, such as e31a/e37a, -e31a/e37b, -e31a/e37a, e37a/-e44, -e31a/-e44 (detected in 70-100% of 8-16 reactions). We found that individual rat cerebellar Purkinje cells also express multiple $Ca_V2.1$ transcript variants, but the range is smaller than in the cerebellum. For example, the combinations -e31a/e37b, e31a/e37a, e31a/e37b were absent from Purkinje cells (detected in 0-12% of 15-20 cells). Furthermore, we did not detect two of the e47 splicing events previously reported in mouse cerebellar Purkinje cells (Tsunemi et al. 2002). These data show that the cerebellar Purkinje cell expresses multiple $Ca_V2.1$ transcripts and suggest that cell-specific regulation of alternative splicing results in a smaller assortment of transcripts in Purkinje cells than in the cerebellum. The data also suggest species-specific control of $Ca_V2.1$ splicing.

Ligon, B., et al., (1998). J. Biol. Chem. 273, 13905-13911.

Soong, T. W., et al., (2002). J. Neurosci. 22, 10142-10152.

Tsunemi, T., et al., (2002). J. Biol. Chem. 277, 7214-7221.

Supported by the MRC and BBSRC.

Where applicable, the experiments described here conform with Physiological Society ethical requirements.

PC144

Effect of slow channel congenital myasthenic syndrome mutation δS268F on human acetylcholine receptor function

R. Lape and D. Colquhoun

Pharmacology, University College London, London, UK

We investigated the effect on receptor function of a naturally occurring congenital myasthenic syndrome mutation S268F in human acetylcholine (ACh) receptor δ subunit. Single channel currents were recorded in cell-attached configuration (at —100 mV transmembrane potential) from HEK293 cells transfected with wild type ACh receptor α, β, ε and δ (or δS268F) subunits. A resolution of 15-25 μs was imposed retrospectively. All means are given ± their standard deviation. The mutant receptors produced longer bursts of openings than the wild type receptors, as expected since this mutation slows endplate current decay. EC_{50}s of 5.3 ± 0.3 μM (wild type) and 0.23 ± 0.01 μM (mutant; n = 3-5 patches per point) were found by fitting the Hill equation to single-channel P_{open} curves. Several mechanisms were fitted by maximising the likelihood of the entire sequence of open and shut time periods, with exact allowance for missed brief events (program HJCFIT; Colquhoun *et al.* 2003). Records obtained at several different ACh concentrations were fitted simultaneously. In order to get good fits, it was essential to include an extra shut state, either distal to the open state (D in scheme 1) or as a proximal 'flip' state (F in scheme 2) (Colquhoun *et al.* 2003; Burzomato *et al.* 2004). For Scheme 2 the gating equilibrium constant or efficacy, $E = \beta/\alpha$, was 34 ± 3 and 54 ± 1 (n = 4 sets) in wild type and mutant receptor, respectively. ACh dissociation rate from diliganded receptor was about 10 times slower for the mutant (1000 ± 1000 s^{-1}; n = 4 sets) than for wild type (9000 ± 6000 s^{-1}; n = 4 sets). Dissociation rate from the 'flipped' conformation (F) in scheme 2 was about 20 times slower for the mutant (300 ± 300 s^{-1}; n = 4 sets) than for wild type (6000 ± 4000 s^{-1}; n = 4 sets,). The last dissociation rate appears to be major contributor to the slowing of the endplate current decay. Other rate constants were not dramatically different between wild type and mutant receptors. The fitted rates predict that δS268F mutation slows the endplate current decay about 15-fold and decreases EC_{50} about 20 times. These effects appear to result mostly from a reduction in ACh dissociation rates.

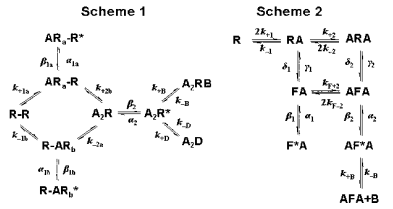

Figure 1. Scheme 1 has a short-lived 'desensitised' state distal to the open state. Scheme 2 includes a change in conformation ('flip') before opening. Both schemes include channel block by ACh. R = shut receptor, R* or F* = open channel, A = ACh, B = blocked channel. F = flipped (but shut) conformation.

Colquhoun et al. (2003) J Physiol 547, 699-728.

Burzomato et al. (2004) J Neurosci 24, 10924-40.

We are grateful to Professor David Beeson and Dr. Martin Brydson (Oxford) for suggesting this project and for supplying much of the DNA.

Where applicable, the experiments described here conform with Physiological Society ethical requirements.

PC145

Role of a non-conserved glycine 'gating hinge' in the second transmembrane domain of heteromeric Kir4.1/Kir5.1 inwardly rectifying potassium channels

L. Shang[1], S. Haider[2] and S.J. Tucker[1]

[1]Oxford Centre for Gene Function, University of Oxford, Oxford, UK and [2]Molecular Biophysics, University of Oxford, Oxford, UK

The mechanisms by which the transmembrane domains of a potassium channel move in order to gate the channel are still not properly understood. A comparison of the 'closed' structure of the KcsA channel and the 'open' state of the MthK channel suggests that the second transmembrane domain hinges at a highly conserved glycine residue (1). This glycine residue is conserved in all known Kv, BK and Kir channels with the exception of Kir5.1 and Kir4.1 which contain either serine or threonine residues at this position. Kir5.1 selectively heteromultimerises with Kir4.1 to form novel heteromeric channels with unique functional and biophysical properties. In particular Kir4.1-Kir5.1 heteromeric channels exhibit a 'bursting' single channel behaviour with multiple subconductance states. In this study we have examined the functional consequences of site-directed mutations at this position in both Kir4.1 and Kir5.1 subunits expressed as a tandemly linked heteromeric channel (Kir4.1-Kir5.1). Wild-type and mutant Kir channel mRNAs were injected into Xenopus oocytes; macroscopic channel properties were examined using two-electrode voltage clamp, whilst single-channel gating was recorded using cell-attached and excised inside-out patches. In comparison to wild-type channels Kir4.1(T154G)-Kir5.1 and Kir4.1(T154G)-Kir5.1(S157G) mutant channels had a reduced open probability (Po= 31.1 ± 8%, n=26 and 26.3 ± 3.4%, n=27, respectively). The recent determination of X-ray crystal structures for the KirBac1.1 channel and the intracellular domains of Kir3.1 combined with the high degree of sequence conservation between different family members enables 3D homology modelling studies to be performed. Using both the KirBac1.1 and Kir3.1 structures as templates we generated a 3D homology model of a heteromeric Kir4.1/Kir5.1 channel and used this model to address the role of this non-conserved gating 'hinge'. The 3D model suggests that the side-chains of residues T154 in Kir4.1 and S157 in Kir5.1 are in close proximity with the pore loops of the channel which form the selectivity filter. Recent studies have indicated that the 'gate' of the Kir channel may involve a complex interaction between the intracellular gate at the 'helix bundle crossing' and a second gate within the selectivity filter. Our studies suggest that these residues may contribute to the unique single-channel properties of Kir4.1-Kir5.1 heteromeric channels by influencing a potential gate within the selectivity filter.

Where applicable, the experiments described here conform with Physiological Society ethical requirements.

PC146

Distribution of the potassium channel subunit Kir6.1 in immortalised cell lines

K. Ng, M. Duchen and A. Tinker

Medicine, UCL, London, UK

The K_{ATP} channel is an octameric protein complex composed of a pore-forming subunit K_{IR} (Kir6.0) and regulatory subunit, the sulphonylurea receptor (SUR). Kir6.1 is proposed to be part of the mitoK_{ATP} channel. The distribution of the Kir6.1 was investigated using fluorescent markers in immortalised cell lines. The C terminus of Kir6.1 was tagged to green fluorescent protein (GFP) using standard molecular biology techniques. HEK-293 and C2C12 cells were transiently transfected with Kir6.1-GFP and an endoplasmic reticulum (ER) marker called ErRed using the liposome based method. Cells were also cotransfected with SUR1. The distribution of Kir6.1 was visualised 36-48 h after transfection using confocal microscopy. The proportion of colocalisation was measured using laserpix software. This calculated the total number of existing green pixels (6.1GFP) that also contained red pixels (Er Red). The results were given as percentages (mean ± S.E.M.) and the Student's t test was used to compare the proportion of colocalisation against a theoretical value of zero. The values obtained were from at least 6 separate transfections. Kir6.1 was found to be predominately located in the ER in both cell lines. C2C12 cells co-transfected with Kir6.1GFP and ErRed showed that about 36 ± 0.025% of Kir6.1 was retained in the ER (n=48) with 36 ± 0.028% also observed in cells co-transfected with SUR1 (n=32). In HEK-293 cells, more Kir6.1 was retained in the ER at 50 ± 0.029% (n=34). Again, there was no change in the distribution of Kir6.1 at 49 ± 0.012% when cells were cotransfected with SUR1 (n=48). Immunofluorescence studies detected the presence of endogenous Kir6.1 in these cell lines using antibodies specific to Kir6.1 and ER marker, concanavalin A. Controls were set up using a preimmune sample and antibody bound onto a fusion protein to which it was raised. In C2C12s, 36 ± 0.022% of Kir6.1 was found in the ER (n=25), with 49 ± 0.020% in HepG2s (n=30) and 45 ± 0.021% in HL-1 cardiomyocytes (n=28). No Kir6.1 was detected in HEK-293 cells.
Colocalisation studies were carried out to see if Kir6.1 existed in the mitochondria. Cells were transfected before they were loaded with 150nm Mitotracker Red. However, the proportion of colocalisation is significantly lower in this experiment in comparison to colocalisation experiment with ErRed. About 26 ± 0.016% of Kir6.1 was found in mitochondria (n=36) and the percentage is not significantly different in the presence of SUR1 28 ± 0.019% (n=17). We conclude that the ATP-sensitive potassium subunit Kir6.1 is predominately distributed in the ER in cardiac and skeletal muscle cell lines, Kir6.1 is also retained in the ER when co-expressed the sulphonylurea receptor. These data show that a small percentage of Kir6.1 may exist in other locations such as the mitochondria.

This work is supported by the British Heart Foundation.

Where applicable, the experiments described here conform with Physiological Society ethical requirements.

PC147

Size-dependent distribution of mechanosensitive nonselective cation channels and regulation by P2Y receptors in rabbit pulmonary arterial myocytes

K. Park, W. Park, Y. Son, S. Kim and Y. Earm

Physiology and Biophysics, Seoul National University College of Medicine, Seoul, South Korea

Active force development by vascular smooth muscle in response to elevation of luminal pressure, or stretch, is termed as the myogenic response, which is independent of neural, metabolic, hormonal, and endothelial factors. Mechanosensitive ion channels, especially
nonselective cation channels (NSC) or chloride channels have been considered as possible candidates for transducing mechanical events into the contractile response of the cell.
We recorded single-channel currents from enzymatically dispersed rabbit pulmonary (PASMCs) and coronary arterial smooth muscle cells (CASMCs) (obtained from humanely killed animals) using the patch clamp technique. With 140 mM CsCl in the pipette solution, application of negative pressures through the pipette induced the activation of channels. The current-voltage relationship was linear in symmetrical ionic conditions, and the single channel conductances for Cs^+, K^+ and Na^+ were 30, 36 and 27 pS, respectively. When $NMDG^+$ was substituted for Cs^+ in the pipette solution, inward currents were abolished whereas outward currents remained active, indicating that the channels were nonselective to cations. The same kind of channels were also observed in mesenteric arterial myocytes.
We also investigated the distribution of mechanosensitive cation channels (NSC_{MS}) in myocytes from pulmonary arteries of various diameters. The open probabilities of NSC_{MS} (NP_O) at 50 mV activated by -10 cmH_2O negative pressure were 0.25 ± 0.18 ($n = 7$) and 0.71 ± 0.23 ($n = 14$) in large-diameter ($\geqq$ 1.5mm, o.d.) and small-diameter ($\leqq$ 600 μm, o.d.) pulmonary arteries, respectively. The chance of recording the NSC_{MS} was higher in small pulmonary arteries than in larger ones (90 vs. 20%). Moreover, the mean numbers of NSC_{MS} in the patch area were 4.45 $\pm$ 1.04 and 1.86 $\pm$ 0.69 in small and larger pulmonary arteries, respectively. Interestingly, the size-dependent distribution and activation of NSC_{MS} were not observed in coronary arteries.
Considering the vaso-regulatory role of ATP released during hypoxic stimuli, we investigated whether the purinergic stimulation affects the activity of NSC_{MS}. When ATP,UTP (1 μM) was included in the pipette for the cell-attached configuration, the NP_O and the chance of recording the NSC_{MS} was largely increased PASMCs while not in CASMCs. However, the bath application of ATP or UTP in the cell-attached configuration had no significant effect on the NSC_{MS}, suggesting a membrane-delimited regulation mechanism.
In summary, we firstly characterized the NSC_{MS} in various arterial myocytes, which could provide a principal mechanism of the myogenic tone generation. In addition, the size-dependent distribution of NSC_{MS} and the positive regulation by purinoceptors (P2Y) suggest that these channels might play a specific role in the regulation of pulmonary circulation, e.g. hypoxic pulmonary vasoconstriction.

Where applicable, the experiments described here conform with Physiological Society ethical requirements.

PC148

Protein kinase A-dependent activation of inward rectifier potassium channels by adenosine in rabbit coronary smooth muscle cells

Y. Son, W. Park, K. Park and Y. Earm

College of Medicine, Physiology, Seoul National University, Seoul, South Korea

Adenosine is an endogenous vasodilator and is believed to play important roles in the regulation of coronary blood flow. Inward rectifier potassium (K_{IR}) channels have been selectively found in small resistance coronary arteries and cerebral arteries. We studied the effect of adenosine on the Ba^{2+}-sensitive K_{IR} channels in the smooth muscle cells isolated from the small-diameter (≤100 μm) coronary arteries of humanely killed New Zealand White rabbit. Adenosine increased K_{IR} currents in concentration-dependent manner (EC50 = 9.4 $\pm$ 1.4 μM, maximum increase of 153%). The adenosine-induced stimulation of K_{IR} current was blocked by adenylate cyclase inhibitor, SQ22536 and was mimicked by adenylate cyclase activator, forskolin. The adenosine-induced increase of current was blocked by cyclic AMP-dependent protein kinase (PKA) inhibitors, KT5720 and Rp-8-CPT-cAMPs. The adenosine-induced stimulation was blocked by an A_3-selective antagonist MRS1334, while the antagonists of other subtypes (DPCPX for A_1, ZM241385 for A_{2A}, and alloxazine for A_{2B}) were all ineffective. Furthermore, an A_3-selective agonist, 2-Cl-IB-MECA induced increase of K_{IR} current. We also examined the effect of adenosine on coronary blood flow (CBF) rate by using the Langendorff-perfused heart. In the presence of glibenclamide to exclude the effects of ATP-sensitive K^+ (K_{ATP}) channels, CBF was increased by adenosine (10 μM), which was blocked by the addition of Ba^{2+} (50 μM). Above results suggest that in rabbit coronary arteries, adenosine increases K_{IR} current via A_3 subtype in a PKA-dependent manner.

Where applicable, the experiments described here conform with Physiological Society ethical requirements.

PC149

Endothelin-1 inhibits inward rectifier K^+ channels in rabbit coronary arterial smooth muscle cells through protein kinase C

W. Park, Y. Son, K. Park and Y. Earm

Physiology and Biophysics, Seoul National University, Seoul, South Korea

We studied inward rectifier K+ (Kir) channels in smooth muscle cells isolated from coronary arteries from humanely killed rabbits. In the cells from small-diameter (< 100 mm, SCASMC) and medium-diameter (100 ~ 200 mm, MCASMC) coronary arteries, Kir currents were clearly identified that were inhibited by Ba2+ (50 mM). By contrast, a very low Kir current density was detected in cells from large-diameter coronary arteries (> 200 mm, LCASMC). The presence of Kir2.1 protein was confirmed in SCASMC from a Western blot assay. Endothelin-1 (ET-1) inhibited Kir currents in a dose-dependent manner, which

was blocked by BQ-123, an ETA receptor antagonist. The inhibition of Kir currents by ET-1 was abolished by pretreatment with the protein kinase C (PKC) inhibitor, staurosporine (100 nM) or GF 109203X (1 mM). The PKC activators, phorbol 12,13-dibutyrate (PDBu) and 1-oleoyl-2-acetyl-sn-glycerol (OAG), reduced Kir currents. ET-1 also inhibited the ATP-dependent K+ (KATP), Ca2+-activated K+ (BKCa), and voltage-dependent K+ (KV) currents, which were not different between SCASMC and LCASMC. In the Langendorff-perfused heart, an application of Ba2+ markedly reduced the coronary blood flow, which was augmented by raising the concentration of extracellular K+ to 15 mM.
From the above results, we conclude that Kir channels are expressed at a higher density in SCASMC than larger arteries, and that the Kir channels activity is negatively regulated by the stimulation of ETA-receptors via PKC pathway. Thus, this response may represent a mechanism by which ET-1 could enhance coronary vasoconstriction in conditions such as coronary vasospasm and hypertension.

Where applicable, the experiments described here conform with Physiological Society ethical requirements.

PC150

Age-related decline in Ca^{2+}-activated K^+ channel activity in human red blood cells

T. Tiffert[1], N. Daw[1], R. Bookchin[2], Z. Etzion[2] and V. Lew[1]

[1]Physiology, University of Cambridge, Cambridge, UK and [2]Medicine, Albert Einstein College of Medicine, New York, NY, USA

As part of a study on red blood cell (RBC) senescence, we investigated whether the activity of endogenous Ca^{2+}-sensitive K^+ channels (Gardos channels) varied with RBC age. RBCs suspended in low-K^+ media and selectively permeabilized to K^+ via Gardos channel activation, rapidly dehydrate by the net loss of KCl and water. When RBC dehydration was followed in time by flow cytometry the Gaussian distribution of volumes was largely retained throughout dehydration (Lew *et al.* 2005), suggesting uniformity of dehydration rates in all cells.
It is well documented that RBCs become denser with age. Therefore, during dehydration, old cells should stay ahead of young cells within the shifting Gaussian distribution. We tested this prediction using glycosylated haemoglobin, Hb A1c, as a reliable age-marker for normal human RBCs.
RBCs suspended in a low-K^+ buffer were Ca^{2+}-loaded in conditions known to generate instant, uniform and maximal Gardos channel activation in the cells (Lew *et al.* 2005). Frequent samples were taken and spun through diethyl phthalate oil, with density 1.117 g/ml, a density not exceeded initially by any RBC. Replacement of 10 mM Cl^- by 10 mM SCN^- in the medium ensured full dehydration of all the cells within 3-4 min. In each sample we measured the percent cells with density above (dense) and below (light) 1.117 g/ml, and their Hb A1c fraction.
Surprisingly, the cells harvested from the first pellets had the lowest Hb A1c (young cells) and those taking longest to become dense had the highest Hb A1c (old cells). This indicated that Gardos channel-mediated dehydration was much more vigorous in the younger RBCs and that retention of the overall Gaussian distribution concealed a substantial age-scrambling of the cells during dehydration.
In conclusion, the results show that Gardos channel activity, measured at saturating Ca^{2+} loads, declines sharply throughout the life-span of human RBCs.
Lew VL *et al.* (2005). *Blood* **105**, 361-367.

Where applicable, the experiments described here conform with Physiological Society ethical requirements.

PC151

Investigation of protein binding partners in heag2 potassium channel

K. Bracey, L. Stevens, C. Tian and D. Wray

Biomedical Sciences, Leeds University, Leeds, UK

We have previously cloned and characterised the human potassium channel, heag2, a member of the ether-a-go-go ion channel family (Ju & Wray, 2002). Besides the usual six membrane-spanning domains, this voltage-activated channel has long intracellular N and C termini. The N terminal region contains a "PAS" domain, thought to be involved in protein-protein interactions, while the C terminal region is even longer and contains a cyclic nucleotide binding domain (cNBD) as well as a number of other domains. The heag2 channel is predominantly expressed in the brain but is also found in skeletal muscle and the heart. In this study, we have looked for binding partners for intracellular regions of the channel. For this, we have made GST fusion proteins of parts of the intracellular regions, and used these to pull down binding partners which we have identified by mass spectrometry.
The GST fusion protein constructs were made by PCR amplification of fragments of intracellular regions, and ligated into pGEX 4T-3 vector with suitable restriction enzymes. The GST fusion proteins were grown in BL21 cells and protein expression induced using IPTG; expression was confirmed using Western blotting with anti-GST antibody. After binding to glutathione beads and washing, the product was mixed with a human brain protein medley (BD Biosciences). Samples were eluted from the beads and run on SDS-PAGE gels; bands were extracted and trypsin digested after staining with Coomassie blue. MALDI-TOF mass spectrometry was then performed to identify the masses of the peptides in the tryptic digests, and then to identify the proteins using Mascot software and protein databases.
A number of binding partners were identified for the C terminal regions of heag2. For the region between the end of S6 to the beginning of the cNBD (475-549), human protein binding partners that were identified were both α and β tubulin as well as a heat shock cognate 71 kDa protein HSP7C. For the region corresponding to the cNBD of heag2 (550-650), binding partners were again α and β tubulin, as well as myelin basic protein. For residues 717-826 of the C terminus, again binding proteins that were identified were α and β tubulin. Finally for the distal part of the C terminus (residues 909-988), myelin basic protein was also identified as a binding partner. Work is in progress to investigate protein binding partners at the N terminus.
In summary, binding partners that were identified fell into several classes, including those concerned with cytoskeletal struc-

ture. However the roles of these proteins in the context of the heag2 channel need to be identified.
M. Ju & D. Wray (2002) FEBS Lett, 524, 204-210.

Work supported by BBSRC.

Where applicable, the experiments described here conform with Physiological Society ethical requirements.

PC152

Endogenous hemichannels play a role in the release of ATP from *Xenopus* oocytes

L. Bahima[1], J. Aleu[1], M. Elias[1], M. Martin-Satue[1], A. Muhaisen[2], J. Blasi[1], J. Marsal[1] and C. Solsona[1]

[1]Pathology and Experimental Therapeutics, Universitat de Barcelona, L'Hospitalet de Llobregat, Barcelona, Spain and [2]Cellular Neurobiology, Parc Cientific de Barcelona, Barcelona, Barcelona, Spain

ATP is an electrically charged molecule required to obtain the energy necessary for cellular activity; in addition, it is a signalling molecule. Usually, the controlled secretion of ATP occurs through the exocytosis of granules and vesicles. However, in some cells, and under certain circumstances, other mechanisms control ATP release. It has been suggested that connexins may be an alternative pathway for ATP release. In gap junctions, connexins link the cytoplasm of two adjacent cells by establishing an intercellular channel and control the passage of ions and molecules up to 1 kDa. The channel is formed by two moieties called hemichannels, or connexins. We have investigated the release of ATP from *Xenopus* oocytes through hemichannels formed by connexin 38 (Cx38), an endogenous, specific type of connexin. Calcium-free solution reversibly activates an inward current (830 ± 202 nA, $p<0.05$) that is inhibited by 1.5 mM octanol (88% inhibition) and 50 μM flufenamic acid (76% inhibition). This calcium-sensitive current depends on Cx38 expression: it is decreased (268 ± 64 nA, $p<0.05$) in oocytes injected with an antisense oligonucleotide against Cx38 mRNA (ASCx38) and is increased in oocytes overexpressing Cx38 (1767 ± 85 nA, $p<0.001$). The opening of Cx38 hemichannels also permeates for small molecules (<1 KDa) like Lucifer Yellow (LY) demonstrating that it is involved in the generation of the inward current generated in the absence of free calcium ions. The activation of the endogenous connexons by calcium-free solution also induced the release of ATP (0.04 ± 0.023 pmol ATP oocyte^{-1} min^{-1}, n = 6), which was inhibited by 50 μM flufenamic acid (61% inhibition), 1.5 mM octanol (66% inhibition) and ASCx38 (72% inhibition) and increased by Cx38 overexpression (300% increase). Altogether, these results strongly suggest that the activation of Cx38 hemichannels is responsible for the release of ATP.

This study was supported by funds from the Ministerio de Ciencia y Tecnologia (DGI) of the Spanish Government, CIRIT of the Generalitat de Catalunya, and Fundacio La Marato de TV3; we are also grateful for the support of Fundacio August Pi i Sunyer.

Where applicable, the experiments described here conform with Physiological Society ethical requirements.

PC153

Investigating the movement of the S4 helix of the HERG potassium channel

D. Elliott and A. Sivaprasadarao

University of Leeds, Leeds, UK

The HERG potassium channel is a voltage-gated potassium (Kv) channel, which plays a key role in the repolarisation of the cardiac action potential. Like all Kv channels, it is a tetramer consisting of a central ion conducting pore domain (S5-P-S6) surrounded by four voltage-sensing domains (S1-S4). However, unlike most Kv channels, HERG conducts the majority of its current upon repolarisation of the membrane. This is attributed to its unique gating properties: during depolarisation, the channel's inactivation gates close before its activation gates begin to open, thereby preventing current flow. During hyperpolarisation, inactivation gates open very rapidly, but the activation gates close so slowly that significant amount of current flows before the activation gates close. The molecular mechanism(s) underlying these unique biophysical properties are far from clear.
Recent studies on the Shaker Kv channel indicate that the voltage sensing S4 segment interacts with S5 of the pore domain and that these interactions may couple voltage sensor motion to the opening and closing of channel gates. Although similar coupling mechanisms can be envisaged for the HERG channel, there is a paucity of information on the membrane-aqueous boundaries of the transmembrane segments to allow investigation of such mechanisms. In this study, we have used substituted cysteine accessibility method to investigate the outer membrane borders of the HERG channel.
HERG channels containing engineered cysteine mutations were expressed in *Xenopus* oocytes and the effect of extracellular application of the membrane-impermeable cysteine modification reagent p-chloromercurybenzenesulfonic acid (pCMBS) on currents was measured using two-electrode voltage clamp.
Application of 100 μM pCMBS to 524C (S4 mutant) abolished the channel activity fully, but only when applied during depolarisation ($n=3$). This indicates that C at 524 moves out of the membrane electric field and becomes exposed to the extracellular solvent during depolarisation. Currents through mutants with cysteines at deeper positions, 527 to 529 of the S4, were also inhibited significantly (55.7±8.9 %, 22.5±4.5 %, 67.8±12.4 % and 47.8±8.5 %, for 526C, 527C, 528C and 529C respectively [mean ± s.e.m.] n=4-7; $p<0.05$, Student's paired t-test). pCMBS, however, has no significant effect on 530C (n=4). These results suggest that the extent of S4 exposure to the extracellular phase is likely to be similar to that of the Shaker channel, and that the first and second positively charged residues in HERG S4 (K525 and R528) align with the first and second positively charged residues in the Shaker S4 (R362 and R365) and not the second and third positively charged residues (R365 and R368) as has been suggested in previous sequence alignments.

Supported by the British Heart Foundation.

Where applicable, the experiments described here conform with Physiological Society ethical requirements.

PC154

The modulatory effect of KNCE1 beta subunits on KCNQ1 K^+ channels is transient

A.N. Poulsen, R. Kofod and D.A. Klaerke

Department of Animal- and Veterinary Basic Sciences, The Royal Veterinary and Agricultural University, DK-1870 Frederiksberg C, Denmark

The one-transmembrane-segment beta-subunit KCNE1 (formerly known as MinK) is known to modulate the characteristics of the voltage-regulated K+ channels of the KCNQ1 type, which are present in various tissues and serves to maintain membrane potential, shape action potentials and transport K+ ions. In heart muscle the combination of KCNE1 and KCNQ1 is essential for proper repolarization during an action potential. It has been hypothesized that KCNE1 forms a protein complex with KCNQ1 in the cell membrane and that the proteins are assembled during synthesis when expressed simultaneously. However, it was recently shown that delayed expression of KCNE1 is still capable of modulating already expressed KCNQ1 channels, suggesting that the coupling of KCNE1 to KCNQ1 can happen in the plasma membrane [1]. KCNE1 and KCNQ1 may have different lifetimes and we therefore asked whether the ion channel characteristics of KCNQ1 channels might change over time after co-expression of KCNQ1 and KCNE1 in Xenopus oocytes as a result of altered relative protein concentrations.
A 1:1 mixture of KCNE1 and KCNQ1 mRNA was injected into Xenopus Laevis oocytes and the maximal KCNQ1 mediated current, voltage dependence and channel activation kinetics was measured daily during the following 14 days. During the first 2-3 days the oocytes expressed a typical KCNE1+KCNQ1 current, but subsequently the current characteristics gradually changed and finally after approx. 9 days the current was not significantly different from pure KCNQ1 currents. The observed change in current characteristics did not seem to be caused by alterations in oocyte condition or interference with endogenous components, as the characteristics of KCNQ1 channels expressed alone changed only very little over time.
In conclusion our experiments suggest that the KCNE beta-subunit over time may be released from the KCNQ1-KCNE complex. This result favors the hypothesis that KCNE subunits act as modulatory molecules, which may be acutely up and down regulated to modulate ion channels already present in the cell membrane.
Grunnet M et al. (2002). J Physiol 542, 119-30.

Where applicable, the experiments described here conform with Physiological Society ethical requirements.

PC155

Physiological mechanisms of lysophosphatidylcholine-induced activation of microglia

T. Schilling[1], C. Stock[2], B. Rueckert[1], F. Lehmann[1], A. Schwab[2] and C. Eder[1]

[1]Institute of Physiology, Berlin, Germany and [2]Institute of Physiology II, Muenster, Germany

Activation of brain macrophages (microglia) occurs rapidly following stimulation with lysophosphatidylcholine (LPC). We identified the physiological mechanisms underlying LPC-induced de-ramification and release of interleukin-1 in the murine microglia cell line BV-2. Patch-clamp experiments revealed activation of non-selective cation currents and Ca^{2+}-dependent K^+ currents by extracellular LPC. LPC-activated non-selective cation channels were permeable for monovalent and divalent cations. They were inhibited by 100 μM Gd^{3+} (n=11), 100 μM La^{3+} (n=10), 500 μM Zn^{2+} (n=4) and Grammostola spatulata venom (diluted 1:2000; n=7), but were unaffected by 100 μM diltiazem (n=7), 50 μM LOE908MS (n=7), 1 mM amiloride (n=7) and 200 μM DIDS (n=7). Ca^{2+} influx through non-selective cation channels caused sustained increases in intracellular Ca^{2+} concentration (n=168). These Ca^{2+} increases were sufficient to elicit charybdotoxin-sensitive Ca^{2+}-dependent K^+ currents (n=21). In LPC-stimulated microglial cells, non-selective cation currents caused transient membrane depolarization, which was followed by sustained membrane hyperpolarization induced by Ca^{2+}-dependent K^+ currents (n=9). Furthermore, 15 μM LPC elicited K^+ efflux by stimulating electroneutral K^+-Cl^- co-transporters, which were inhibited by 1 mM furosemide and 100 μM DIOA (n=4 experiments). LPC-induced morphological changes (de-ramification) were Ca^{2+}-independent (n=150). They were prevented by simultaneous inhibition of non-selective cation channels and K^+-Cl^- co-transporters (n=314; $p<0.001$). In contrast, Ca^{2+} influx through non-selective cation channels was required for LPC-induced release of interleukin-1 from microglial cells (n=4 experiments; $p<0.001$). Microglial IL-1 release was inhibited by 200 nM charybdotoxin (n=4 experiments; $p<0.05$), but was unaffected by 1 mM furosemide (n=4 experiments). These data suggest that distinct physiological mechanisms are involved in LPC-induced microglial activation.

Supported by the Deutsche Forschungsgemeinschaft grants SFB 507/C7, GRK 238 and a Heisenberg fellowship (all to C.E.) and Schw 407/9-1 (to A.S.).

Where applicable, the experiments described here conform with Physiological Society ethical requirements.

PC156

Differential binding kinetics between *Shaker*-related Kv1 channels and the Kvβ1 regulatory protein

R. Ginham, S. Stafford, A.R. Davies, S. Kanumilli and R.Z. Kozlowski

Department of Pharmacology, School of Medical Sciences, University of Bristol, Bristol, BS8 1TD, UK

Functional voltage-gated K_+ (Kv) channels exist as homomeric or heteromeric tetramers of Kv α subunits that form the channel 'pore'. The kinetics of *Shaker*-type Kv (Kvα 1.x) channel currents can be specifically modulated by accessory proteins know as Kvβ subunits that bind to Kv1.x subunit counterparts through N-terminal region known as the 'T1' domain (Gulbis *et al.* 2000). Since Kvβ subunits have been demonstrated to differentially modulate Kvα 1.x channel kinetics (Sewing *et al.* 1996), this study aimed to determine the binding kinetics between Kvα 1.1, Kvα 1.2, Kvα 1.3, Kvα 1.5 & Kvα 1.6 T1 domains to the Kv β1 'core' protein.
rKv β1 core proteins were cloned from whole brain tissue samples obtained from humanely killed rats, and a sequence encod-

ing an affinity tag (biotin carboxyl carrier protein) incorporated into the cDNA. rKv β1 core proteins were subsequently expressed in *E. coli* and immobilised onto streptavidin substrates via the affinity tag, through a biotin-streptavidin interaction. rKvα 1.x T1 domains were cloned from rat whole brain cDNA samples, expressed in *E. coli*, purified and labelled with Cy3 dye.
Binding studies were conducted by quantitative fluorescent measurement of Cy-3 labelled rKv 1.x T1 αdomain binding to immobilised rKv β1 core proteins. Analyses of the binding parameters were carried out using conventional methodologies (Davies *et al.* 1999) and are summarised in Table 1.
These results show that rKv α1.x T1 domains display differential binding kinetics to immobilised rKv β1 subunits as demonstrated by the differences in equilibrium dissociation constants and rates of association. The differential binding affinity of rKvα 1.x T1 domains to rKv β1 subunits may underlie the differential functional modulation of native rKv 1.x currents by rKv β1 subunit accessory proteins and ultimately facilitate the characterisation of a novel mode of modulating Kv1.x channels in a subtype selective manner.

rKvα 1.x T1	*K_d (nM)*	*K_{obs} (min^{-1})*	*$t_{1/2}$ (min)*
1.1	*105 ± 10*	*0.053*	*13.1*
1.2	*72 ± 4*	*0.026*	*27.1*
1.3	*128 ± 13*	*0.022*	*26.4*
1.5	*86 ± 5*	*0.023*	*28.1*
1.6	*175 ± 14*	*0.026*	*22.6*

Table 1. Binding parameters of rKvα 1.x T1 domains to immobilised Kv β1 core proteins (n = 3). K_d, equilibrium dissociation constant; K_{obs}, observed association rate constant; $t_{1/2}$, amount of time required for the ligand to occupy 50% of the binding sites.

Davies ARL, Hardick DJ, Blagbrough IS, Potter BV, Wolstenholme AJ & Wonnacott S (1999). Neuropharmacology 38, 679-690.

Sewing S, Roeper J & Pongs O (1996). Neuron 16, 455-463.

Gulbis JM, Zhou M, Mann S & MacKinnon R (2000). Science 289, 123-127.

This work was funded by Lectus Therapeutics Limited of which Roland Z. Kozlowski is CEO.

Where applicable, the experiments described here conform with Physiological Society ethical requirements.

PC157

Functional expression of neuronal voltage-gated sodium channels in neonatal rat ventricular cardiomyocytes

C. Zechner[1], S. Bischoff[1], M.L. Koller[1], J. Muck[1], E. Wischmeyer[2], A. Maass[1] and S. Maier[1]

[1]Department Internal Medicine I / Center of Cardiovascular Medicine, University Wuerzburg, Wuerzburg, Germany and [2]Institute of Physiology II, University Wuerzburg, Wuerzburg, Germany

Gaughan JP et al. (1998). Am J Physiol 275, H577-590.

Maier et al. (2002). PNAS 99, 4073-4078.

Where applicable, the experiments described here conform with Physiological Society ethical requirements.